NASA TECHNICAL NOTE

NASA TN D-6630

COMPUTER EXPERIMENTS ON THE STRUCTURE AND DYNAMICS OF SPIRAL GALAXIES

by Frank Hohl

Langley Research Center
Hampton, Va. 23365

NATIONAL AERONAUTICS AND SPACE ADMINISTRATION • WASHINGTON, D. C. • MARCH 1972

1. Report No.	2. Government Accession No.	3. Recipient's Catalog No.
NASA TN D-6630		

4. Title and Subtitle	5. Report Date
COMPUTER EXPERIMENTS ON THE STRUCTURE AND DYNAMICS OF SPIRAL GALAXIES	March 1972
	6. Performing Organization Code

7. Author(s)	8. Performing Organization Report No.
Frank Hohl	L-8109
	10. Work Unit No.
9. Performing Organization Name and Address	112-02-22-01
NASA Langley Research Center Hampton, Va. 23365	11. Contract or Grant No.
	13. Type of Report and Period Covered
12. Sponsoring Agency Name and Address	Technical Note
National Aeronautics and Space Administration Washington, D.C. 20546	14. Sponsoring Agency Code

15. Supplementary Notes

16. Abstract

The evolution of an initially balanced rotating disk of stars with an initial velocity dispersion given by Toomre's local criterion is investigated by means of a computer model for isolated disks of stars. It is found that the disk is unstable against very large-scale modes. After about two rotations the central portion of the disk tends to assume a bar-shaped structure. A stable axisymmetric disk with a velocity dispersion much larger than that given by Toomre's criterion is generated. The final mass distribution for the disk gives a high-density central core and a disk population of stars that is closely approximated by an exponential variation.

Various methods and rates of cooling the hot axisymmetric disks were investigated. It was found that the cooling resulted in the development of two-arm spiral structures which persisted as long as the cooling continued. An experiment was performed to induce spiral structure in a galaxy by means of the close passage of a companion galaxy. Parameters similar to those expected for M51 and its companion were used. It was found that because of the rather high velocity dispersion of the disturbed disk galaxy, only a weak two-arm spiral structure appeared as the result of the passage. The evolution of a uniformly rotating disk galaxy which is a stationary solution of the collisionless Boltzmann equation is investigated for various values of the initial rms velocity dispersion. It is found that the disk becomes stable at a value of the velocity dispersion predicted by theory.

17. Key Words (Suggested by Author(s))	18. Distribution Statement
Galactic dynamics Spiral structure Computer experiments	Unclassified – Unlimited

19. Security Classif. (of this report)	20. Security Classif. (of this page)	21. No. of Pages	22. Price*
Unclassified	Unclassified	50	$3.00

*For sale by the National Technical Information Service, Springfield, Virginia 22151

COMPUTER EXPERIMENTS ON THE STRUCTURE AND DYNAMICS OF SPIRAL GALAXIES

By Frank Hohl
Langley Research Center

SUMMARY

The evolution of an initially balanced rotating disk of stars with an initial velocity dispersion given by Toomre's local criterion is investigated by means of a computer model for isolated disks of stars. It is found that the disk is unstable against very large-scale modes. After about two rotations the central portion of the disk tends to assume a bar-shaped structure. A stable axisymmetric disk with a velocity dispersion much larger than that given by Toomre's criterion is generated. The final mass distribution for the disk gives a high-density central core and a disk population of stars that is closely approximated by an exponential variation.

Various methods and rates of cooling the hot axisymmetric disks were investigated. It was found that the cooling resulted in the development of two-arm spiral structures which persisted as long as the cooling continued.

An experiment was performed to induce spiral structure in a galaxy by means of the close passage of a companion galaxy. Parameters similar to those expected for M51 and its companion were used. It was found that because of the rather high velocity dispersion of the disturbed disk galaxy, only a weak two-arm spiral structure appeared as the result of the passage.

The evolution of a uniformly rotating disk galaxy which is a stationary solution of the collisionless Boltzmann equation is investigated for various values of the initial rms velocity dispersion. It is found that the disk becomes stable at a value of the velocity dispersion predicted by theory.

INTRODUCTION

With the introduction of computer models for thin self-gravitating stellar systems, the field of experimental stellar dynamics is beginning to provide fresh insights into the structures of spiral galaxies. Two computer models for self-consistent disk galaxies

have recently been described, and to a certain extent demonstrated, by Miller and Prendergast (ref. 1) and by Hohl and Hockney (ref. 2.).

To investigate the development of spiral structure, the model was modified by Hohl (refs. 3 and 4) to include a fixed central force similar to the Schmidt model of the Galaxy. It was then found that spiral structure persisted for more than eight rotations. Miller, Prendergast, and Quirk (ref. 5) have also modified their model to include a dissipative component resembling gas. They found that some very interesting spiral patterns developed, especially in the "gas" component, and that such patterns remained for about three galactic rotations. Such a combined system of stars and gas seems more realistic for the study of the spiral phenomena than a model composed only of stars.

However, a basic understanding of the structure of galaxies clearly requires a knowledge of how purely stellar disks would behave. Accordingly, the present report will be concerned primarily with the dynamical evolution of isolated disks consisting of stars alone. The computer model used for the calculations is that developed by Hohl and Hockney (ref. 2). From previous work (refs. 3 and 6 to 9) it is, of course, already clear that disks of stars with velocity dispersions less than those estimated by Toomre (ref. 6) to be locally stabilizing are violently unstable. For this reason the present paper reports primarily on disks with initial velocity dispersions at least equal to those given by Toomre's local criterion. In a previous paper (ref. 9) the authors were overenthusiastic in calling such disks stable. It would have been more appropriate to say that only the fast-growing small-scale gravitational instabilities are avoided when Toomre's criterion is satisfied. As will be seen herein, such disks remain susceptible to slower large-scale instabilities, primarily of the bar-making type.

Thus, disks of stars are considerably more difficult to stabilize than indicated by local analyses. It is, of course, only with the advent of computer experiments such as those described here that it has become possible to determine the behavior of disks of stars in the large. Before such experiments, there existed no really adequate theory describing the overall dynamics of disks of stars.

Freeman (ref. 10) has summarized the observational evidence that most spiral and SO galaxies have a dense spheroidal central component and a disk component of stars described by an exponential light distribution. One of the questions the present report tries to answer is whether a disk of stars will evolve to a similar final state.

In published work (refs. 1, 2, 3, 5, and 9) on the simulation of disk galaxies, the initial conditions chosen were not solutions of the time-independent collisionless Boltzmann equation. Even though some of the initial conditions (refs. 3 and 9) were for initially balanced disks, these initial conditions did not correspond to stationary disks. One exception to this is the "cold" balanced disk, which, however, is violently unstable. In the

present paper the evolution of initially stationary disks for various temperatures is investigated.

The computer model used for the calculations is described in the appendix.

How striking the resemblance of computer-simulated disk galaxies is to actual galaxies is shown in figure 1. In that figure four computer-generated galaxies are compared with photographs of actual galaxies.

SYMBOLS

E	total energy
f	distribution function
G	gravitational constant
H	Green's function
J	angular momentum
K	gravitational field, $\nabla\phi$
$M_\odot$	mass of Sun
m	mass
N	dimension of array used in potential calculations
$n = N/2$	
$Q = \sigma_r/\sigma_{r,min}$	
R	radius of disk galaxy
r,θ,z	cylindrical coordinates
T_0	rotational period of cold balanced disk
t	time

V	rotational velocity
v	velocity
x,y,z	Cartesian coordinates
$\delta(z)$	Dirac delta function
κ	epicyclic frequency
μ	surface mass density
σ	velocity dispersion
$\sigma_{r,min}$	velocity dispersion defined by equation (3)
ϕ	gravitational potential
ω	angular velocity
ω_o	angular velocity of cold balanced disk

Subscripts:

i,j	summation indices
k,l	summation indices
max	maximum
r,θ	radial and azimuthal component
x,y	summation indices

Notation:

~	Fourier transformed quantity

EVOLUTION OF AN INITIALLY BALANCED UNIFORMLY ROTATING DISK

In the following sections the evolution of a balanced uniformly rotating disk of stars with an initial velocity dispersion given by Toomre's local criterion (ref. 6) is investigated. Disks with other initial mass distributions have previously been investigated in less detail (ref. 3).

Initial Conditions

The present report describes in detail the evolution of a balanced uniformly rotating disk of stars with an initial velocity dispersion given by Toomre's local criterion. The surface mass density of the uniformly rotating disk is given by

$$\mu(r) = \mu(0)\sqrt{1 - \frac{r^2}{R^2}} \tag{1}$$

where r is the radial coordinate, R is the radius of the disk, and $\mu(0)$ is the central surface mass density. The uniform angular velocity required to balance the cold (zero-velocity-dispersion) disk is

$$\omega_o = \pi\sqrt{\frac{G\mu(0)}{2R}} \tag{2}$$

where G is the gravitational constant.

Toomre's local criterion (ref. 6) for suppression of all axisymmetric instabilities requires a minimum radial velocity dispersion (Gaussian velocity distribution) given by

$$\sigma_{r,min} = 3.36\,\frac{G\mu}{\kappa} \tag{3}$$

where σ_r^2 is the second moment of the distribution function, μ is the local value of the density, and κ is the local value of the epicyclic frequency. The epicyclic frequency is defined by

$$\kappa^2 = \frac{\partial K_r}{\partial r} + \frac{3K_r}{r} \tag{4}$$

where K_r is the radial component of the gravitational field. For the uniformly rotating disk $K_r = \omega_o^2 r$; thus, $\kappa = 2\omega_o$ and

$$\sigma_{r,min} = 0.341 R\omega_o \sqrt{1 - \frac{r^2}{R^2}} \tag{5}$$

To determine whether Toomre's criterion will stabilize the disk, the initial (Gaussian) velocity dispersion is taken as

$$\sigma_r(r) = \sigma_{r,min} \tag{6}$$

for the radial component and

$$\sigma_\theta(r) = \frac{\kappa(r)}{2\omega_o(r)} \sigma_{r,min} \tag{7}$$

for the azimuthal component. For the uniformly rotating disk, equations (6) and (7) become

$$\sigma_r(r) = \sigma_\theta(r) = 0.341 R\omega_o \sqrt{1 - \frac{r^2}{R^2}} \tag{8}$$

Because of the added velocity dispersion the initial angular velocity of the stars ω for a balanced disk is lower than ω_o. By summing the forces acting on a small surface element of the disk, the following equation is obtained:

$$\omega^2 = \omega_o^2 + \frac{1}{r\,\mu(r)} \frac{\partial}{\partial r}\left[\mu(r)\sigma_r^2(r)\right] + r^{-2}\left[\sigma_r^2(r) - \sigma_\theta^2(r)\right] \tag{9}$$

For the uniformly rotating disk, equation (9) gives $\omega = 0.809\omega_o$, which results in a circular velocity given by

$$V_\theta = 0.809 r\omega_o \tag{10}$$

The initial conditions do not exactly satisfy the collisionless Boltzmann equation for a stationary stellar disk. An initial condition with a Gaussian velocity distribution was preferred to the stationary initial state corresponding to the density given by equation (1), because Toomre's criterion is strictly valid only for Gaussian velocity distributions. The stationary state for the uniformly rotating disk (ref. 11) has a peculiar non-Gaussian velocity distribution such that the density in phase space is not a decreasing function of epicyclic amplitude; hence overstabilities may be present (ref. 12). With the exception of the uniformly rotating disk, there is a rather unfortunate lack of exact, hot equilibrium models for disks of stars.

The initial distribution of stars is generated by means of a pseudorandom-number generator. The initial circular velocity is given by equation (10), and superposed on the circular velocity is a velocity dispersion with a Gaussian distribution corresponding to $\sigma_{r,min}$ as given by equation (8).

Axisymmetric Evolution

Since the initial state chosen for the model is not an equilibrium state, the axisymmetric behavior of the disk is first investigated to determine whether any axisymmetric instabilities or other misbehavior might be present. This is done by considering the evolution of the initial disk under a gravitational field that is constrained to remain purely radial. This gravitational field is obtained by averaging at each time step the fields computed in the $\pm x$-directions and the $\pm y$-directions. The results are shown in figure 2 for eight rotations. Initially the disk has an arbitrarily chosen radius of 8 kpc. The square border enclosing the disk is then at $x = \pm 19$ kpc and $y = \pm 19$ kpc and covers only part of the 128×128 square array of cells used for the gravitational-field calculations. Each of the 100 000 stars in the disk can be thought of as having a mass of $0.84 \times 10^6 M_\odot$. The time shown in figure 2 and in subsequent figures is in units of the rotational period of the cold balanced disk; each such unit equals 1.5×10^8 years.

The disk shown in figure 2 remains, of course, axisymmetric. After a few small pulsations it settles down to an essentially steady state. When the total kinetic energy of the disk is plotted as a function of time, the initial amplitude of the oscillations in the total kinetic energy is about 8 percent of the mean value. These oscillations in the total kinetic energy are quickly damped; after four rotations the amplitude of the oscillations is less than 1 percent of the mean value. Figure 3 shows the evolution of the density. Again it can be seen that the system quickly reaches a steady state. During the evolution of the disk, the value of $\sigma_r/\sigma_{r,min}$ remains near unity for r less than 5 kpc. These results show that any troubles the disk may have are basically nonaxisymmetric in nature.

The disk in figure 2 at $t = 8$ should now be very close to a stationary state of the collisionless Boltzmann equation. If the evolution of the disk is continued without the constraint of keeping the gravitational field radial, the evolution shown in figure 4 is obtained. In less than two additional rotations the disk assumes a bar-shaped structure – an indication that the newly made equilibrium is unstable in a nonaxisymmetric sense.

Fully Nonaxisymmetric Evolution

These instabilities are now studied by returning to the smooth but slightly nonequilibrium disk that was the starting point for figure 2. Those initial conditions, by the way, are such that the virial theorm is satisfied – that is, the negative of the calculated poten-

tial energy equals twice the kinetic energy with an accuracy of about 0.5 percent. This small discrepancy is meaningless because of the approximate method used for calculating the potential energy (ref. 2). Also, the maximum change in the calculated total energy of the system during its evolution is near 1 percent, and the variation in the total angular momentum is even less.

The totally unconstrained evolution of this disk is displayed in figure 5. It shows that the disk is indeed stabilized against small-scale disturbances which would completely disrupt a cold disk in less than one rotation (ref. 3). However, it is again found that the disk is not stabilized against relatively slow-growing large-scale disturbances which cause the system to assume a very pronounced bar-shaped structure after two rotations. After about four rotations the disk population of stars constitutes a nearly axisymmetric distribution surrounding a dense central oval or bar-shaped core. The oval contains nearly two-thirds of the total mass of the disk and has an axis ratio of about 3:2. After about four rotations there is little change in the structure of the disk, and the bar rotates with a constant period of 2.25 times the period of the cold balanced disk.

To obtain more quantitative information on the structure and evolution of the bar-shaped central part of the system, a number of annular rings 1 kpc in width and concentric with the disk were superposed on the disk shown in figure 5. Each annular ring was divided into 100 equal segments, and the number of stars in each segment was determined. The results are shown in figure 6 for annuli centered at the three radii shown. The fluctuations caused by generating the initial positions of the stars by means of a random-number generator can be seen for the curves at $t = 0$. At this time there are no stars in the annulus at $r = 10$ kpc because the initial disk has a radius of only 8 kpc. After one rotation the bar structure begins to form and stars are ejected beyond the 10 kpc radius. At $t = 2.0$ the bar is very pronounced, and after this time it begins to broaden. After eight rotations the disk has assumed a steady state, as indicated by the result that neither the amplitude nor the structure of the rotating bar changes any longer.

To picture the radial variation of parameters describing the disk, the disk was divided into a number of concentric rings each 0.5 kpc in width. The radial dependence of various parameters averaged azimuthally over each ring was then obtained. Figure 7 shows the radial variation of the rms radial-velocity dispersion obtained in that manner. At $t = 0$ the radial velocity dispersion is described by equation (5). As high-velocity stars are ejected radially outward, the velocity dispersion becomes large for large radii. After about eight rotations the velocity dispersion remains essentially unchanged. In interpreting the results shown in figure 7 and in subsequent figures, the nonaxisymmetric shape of the disk for small radii ($r < 8$ kpc) should be kept in mind. A better indication of how hot the stars in the disk are can be obtained from a plot of the azimuthally averaged value of

$$Q = \frac{\sigma_r(r)}{\sigma_{r,min}}$$

(The value of $\sigma_{r,min} = 3.36\ G\mu/\kappa$ is obtained by using μ as given in fig. 9 and by obtaining κ from the slope of K_r.) The radial dependence of Q is shown in figure 8. Initially Q is given a value near 1. However, as the disk evolves, Q increases rapidly in the outer regions of the disk. Figure 8 is typical of the high velocity dispersion in the outer parts of the disk for computer-generated galaxies. For a number of other initial conditions (ref. 3), typical values of Q were found to be between 2 and 4.

The evolution of the surface mass density is shown in figure 9. It can be seen from this figure that the central mass density increases by about a factor of 4 during the 11.6 rotations shown. After eight rotations the radial variation in density changes only very little. To determine how closely the final density variation corresponds to an exponential variation, the density for $t = 8$ and $t = 11.6$ rotations is plotted in figure 10 on a semilog scale. This distribution of the disk population of stars (outside $r = 8$ kpc) is closely approximated by an exponential variation with a scale length of 8.6 kpc. In the high-density central oval the density also closely follows an exponential law, but with the much shorter scale length of 1.44 kpc. Figure 10 also illustrates how little the structure of the disk changes during the last 3.6 rotations. The density functions shown in figures 9 and 10 represent the azimuthally averaged value. In figure 11 is presented the unaveraged density at $t = 8$ along the bar and across the bar. As expected, the density falls off faster across the bar than it does along the bar. For radii greater than about 10 kpc the densities in the two directions are essentially the same.

GENERATION OF A STABLE AXISYMMETRIC DISK

It was found that disks of stars with initial conditions generated according to analytical expressions such as equations (1) to (10) are generally unstable and finally assume a steady state with a central bar-shaped structure. The evolution of such warm disks is found to be very similar, irrespective of whether the initial mass distribution is Gaussian, exponential, or some other distribution (ref. 3). Also, the stationary state finally reached by the disks results in a very hot population of stars in the outer part of the disk, as is shown in figure 8. In order to generate an axisymmetric stable disk, the final distribution of stars (at $t = 11.6$) of the disk shown in figure 5 was used as an initial condition after symmetrizing out the bar structure. All stars kept the same (radial and tangential) velocity components and radius, but they were redistributed randomly in longitude. This new disk has the same radial variation of its different parameters as given (at $t = 11.6$) in figures 5, 7, 8, 9, and 10.

The reason for using this highly artificial procedure of "symmetrizing" was mainly to show that the bar structure, although here persistent, is not necessarily very strong or "deep." Figure 12 depicts the evolution of the new disk for six rotations. The disk is now axisymmetric and stable; all parameters remain essentially constant during the evolution. For example, the variation of the density given in figure 13 shows no change between two and six rotations. Note also that the "experimentally" obtained density variation is closely approximated by the sum of the exponentials

$$\mu(r) = 4.2 \times 10^9 \exp\left(-\frac{r}{1.44}\right) + 3.6 \times 10^7 \exp\left(-\frac{r}{8.6}\right) \tag{11}$$

Since the disk is axisymmetric and stable, the variation of its rms velocities near a fixed radius should provide information on collisional or thermalization effects that may be present in the model. In figure 14 the rms velocities of stars in a 0.5-kpc-wide ring centered at the four radii shown are plotted as a function of time. It can be seen that there is no systematic increase (or decrease) in the rms velocities for the six rotations shown.

Figure 15 shows the radial dependence of the mean circular velocity of the stars $\langle V_\theta \rangle$, of $\omega = \sqrt{K_r/r}$, and of $r\omega$. It is interesting to note that the azimuthally averaged radial dependence of the parameters of the disk did not change after the central bar structure was eliminated by symmetrizing. The values of Q for the axisymmetric disk are the same as shown in figure 8 at $t = 11.6$ and are rather high. For some of the disks investigated, final values of Q near 2 were obtained. However, for most of the disks investigated (ref. 3) the final value of Q is near 4.

COOLING OF THE AXISYMMETRIC DISK

The stable axisymmetric disk described in the previous section is rather hot, especially in the outer regions of the disk. It is therefore of interest to determine the effects of cooling the disk. Various methods of cooling were tried. For example, during each rotation a certain percentage (from 5 to 30 percent) of the stars, chosen at random, had a portion of their noncircular velocities removed in proportion to their radii. Thus stars near the center kept nearly all their random motion whereas stars far away from the center were placed in more nearly circular orbits. Another method, somewhat more analogous to the "gas collisions" of Miller et al. (ref. 5) was simply to place a certain percentage of the stars during each rotation into purely circular orbits. All methods of cooling which were tried gave essentially the same results.

Figure 16 shows the effects of cooling when for each rotation 10 percent of the stars are selected at random and are placed in circular orbits. The initial disk is that shown in figure 12 at $t = 6$. During the first three rotations the appearance of the disk changes

little. However, at $t = 3.1$ there is already a pronounced bar structure at $r = 2.5$ kpc. After $t = 3.1$ a two-arm structure appears, which during the following 1.5 rotations displays a theta-shaped structure. After $t = 4.5$ the spiral structure opens up and rotates with a fairly constant speed of about 10 km s^{-1} kpc^{-1}. This compares with a mean circular velocity of the stars of about 15 km s^{-1} kpc^{-1} at $r = 10$ kpc. These results tend to support the density-wave theory of Lin (ref. 13). At $t = 6$ the value of Q for the disk was between 2 and 3. Any further cooling only caused the collective instabilities to heat up the disk as fast as it was being cooled. This effect can be seen in figure 17 where the radial velocities of the stars are plotted as a function of radius. At $t = 2$ the effect of placing a number of stars in purely circular orbits is clearly visible by the concentration of stars with zero radial velocity. At $t = 4$ an increased velocity dispersion corresponding to the condensation of stars in the theta-shaped spiral arms is clearly visible. Also, the effects of heating by means of collective instabilities prevent a reduction of the radial velocity dispersion after $t = 6$. Figure 18 displays the azimuthal variation of the number density at three radii. These results show that in addition to the density-wave-like spiral structure of the outer disk, the galaxy also develops a strong barlike structure of the central core.

The results of removing a portion of the stars' random velocity in proportion to the star's radial distance is shown in figure 19. Thirty percent of the stars are affected during each rotation. The results are slightly different from those of figure 16, primarily because the cooling rate is now larger. In fact cooling proceeds now so rapidly that at $t = 11$ clusters of stars have condensed and are circling the central core as satellites.

EFFECT OF SATELLITE GALAXY

Alar Toomre of the Massachusetts Institute of Technology has studied a number of spiral galaxies and found that many have nearby companion galaxies. To determine the effect of a close passage, a stable axisymmetric disk galaxy similar to that shown in figure 12 was perturbed by the passage of a companion galaxy having one-fourth the mass of the primary galaxy. The parameters for M51 were chosen for the calculations. The orbit was direct, the inclination of the companion's orbit plane to the plane of the primary galaxy was 75°, the angle between the node and periapsis was 20°, and periapsis was 25 kpc. The effect of the passage on the structure of the primary galaxy is shown in figure 20. The time is given in rotational periods of the primary galaxy; $t = 0$ corresponds to the time at periapsis. These results indicate that only a weak two-arm spiral structure developed. This was to be expected since the velocity dispersion of the primary galaxy is rather high, as shown in figure 21. The value of Q ranges from about 2 in the central region to 6 in the outer disk. A more detailed view of the velocity distribution is given in figure 22, where the radial velocity distribution for the stars in various annular

rings is given. The effect of the large random velocities on the formation of spiral structure can be determined by plotting the distribution of stars in various velocity intervals. This is done in figure 23. As can be seen, the spiral structure is quite pronounced for the lower velocities, but can hardly be detected for the higher velocities. This was to be expected since the large random velocities have a dispersive effect on the formation of spiral structure. It thus appears that a much cooler primary galaxy is needed to study the effects of a close passage.

SELF-CONSISTENT STATIONARY DISKS

Presently, there are no really "good" stationary solutions of the collisionless Boltzmann equation available for disk galaxies. For certain mass distributions analytical stationary solutions can be obtained; however, these solutions have certain undesirable features (e.g., the distribution function becomes singular at the edge of the disk) which make them unlike any "real" galaxy. Nevertheless, there are analytical predictions as to the stability and behavior of such disks. Thus, by investigating such stationary states, it is possible to determine whether the analytical methods used to study the behavior of disk galaxies yield the correct predictions.

Theory

A time-independent, axisymmetric self-consistent disk of stars is described by the collisionless Boltzmann equation

$$v_r \frac{\partial f}{\partial r} + \frac{v_\theta^2}{r} \frac{\partial f}{\partial v_r} - \frac{v_r v_\theta}{r} \frac{\partial f}{\partial v_\theta} + K_r \frac{\partial f}{\partial v_r} = 0 \tag{12}$$

where v_r and v_θ are the radial and azimuthal velocity components and $f(r,v_r,v_\theta)$ is the distribution function defined so that

$$dm = f(r,v_r,v_\theta) dv_r \, dv_\theta r \, dr \, d\theta \tag{13}$$

corresponds to the mass in a phase-space element within the surface element $r \, dr \, d\theta$. The gravitational field K_r equals $\frac{\partial \phi}{\partial r}$, where the potential $\phi(r,z)$ is obtained from the Poisson equation

$$\nabla^2 \phi = 4\pi G \, \mu(r) \, \delta(z) \tag{14}$$

where G is the gravitational constant and the density $\mu(r)$ is given by

$$\mu(r) = \iint f(r,v_r,v_\theta)dv_r\, dv_\theta \tag{15}$$

According to Jeans' theorem (refs. 14 and 15), any function of the form

$$f(r,v_r,v_\theta) = f(E,J) \tag{16}$$

is a solution of equation (12), where the energy E and the angular momentum J are given by

$$E = \frac{1}{2}\left(v_r^2 + v_\theta^2\right) + \phi$$

and

$$J = rv_\theta$$

An axisymmetric mass-density variation for which the corresponding distribution function can be obtained is that for the uniformly rotating disk

$$\mu(r) = \mu(0)\sqrt{1 - \frac{r^2}{R^2}}$$

where $\mu(0)$ is the central mass density and R is the radius of the disk. The gravitational potential inside the disk is (ref. 3)

$$\phi(r) = \frac{1}{2}\omega_o^2 r2 - \omega_o^2 R^2 \tag{17}$$

where $\omega_o = \pi\sqrt{G\mu(0)/2R}$ is the uniform angular velocity required to balance the cold (zero-velocity-dispersion) disk. Omitting the constant term in equation (17) gives

$$2E = \omega_o^2 r2 + v_r^2 + v_\theta^2 \tag{18}$$

Consider now a distribution function of the form

$$f(E,J) = C_1\left(C_2 - 2E + 2\omega J\right)^{-1/2} \tag{19}$$

where ω is the constant angular velocity of the disk, constrained so that $0 \leqq \omega \leqq \omega_o$. This requires that

$$C_2 - 2E + 2\omega J \geqq 0$$

Thus, for $r = R$, $v_r = 0$, and $v_\theta = R\omega$,

$$C_2 - \omega_o^2 R^2 - \omega^2 R^2 + 2\omega^2 R^2 = 0$$

or

$$C_2 = \left(\omega_o^2 - \omega^2\right)R^2 \tag{20}$$

Substituting for E, J, and C_2 allows equation (19) to be written as

$$f(E,J) = C_1\left[\left(\omega_o^2 - \omega^2\right)R^2 - 2E + 2\omega J\right]^{-1/2}$$

$$= C_1\left[\left(\omega_o^2 - \omega^2\right)\left(R^2 - r^2\right) - v_r^2 - \left(v_\theta - r\omega\right)^2\right]^{-1/2}$$

From equation (15),

$$\mu(r) = \iint f(E,J)dv_r\, dv_\theta = 2\pi R C_1 \sqrt{\omega_o^2 - \omega^2}\sqrt{1 - \frac{r^2}{R^2}}$$

Therefore, since $\mu(r) = \mu(0)\sqrt{1 - \frac{r^2}{R^2}}$, the following equation is obtained:

$$C_1 = \frac{\mu(0)}{2\pi R\sqrt{\omega_o^2 - \omega^2}}$$

and

$$f(E,J) = f\left(r,v_r,v_\theta\right) = \frac{\mu(0)}{2\pi R\sqrt{\omega_o^2 - \omega^2}}\left[\left(\omega_o^2 - \omega^2\right)\left(R^2 - r^2\right) - v_r^2 - \left(v_\theta - r\omega\right)^2\right]^{-1/2} \tag{21}$$

The distribution function (21) is a stationary solution of the Boltzmann equation (12). In equation (21) $\omega = \omega_o$ corresponds to the cold, violently unstable disk which was previously investigated (refs. 2 and 3). For $\omega = 0$ the disk is nonrotating and purely pressure supported.

Toomre (ref. 6) estimated that for a disk with a Gaussian velocity distribution, a velocity dispersion equal to or greater than

$$\sigma_{r,min} = 3.36\,\frac{G\mu}{\kappa}$$

should be locally stabilizing for exponentially growing axisymmetric modes. Toomre's evaluation of $\sigma_{r,min}$ is not easily extended to the present non-Gaussian velocity distribution given by equation (21). Also, overstabilities may be present since the density of stars in phase space is not a decreasing function of epicyclic amplitude (ref. 12). Nevertheless, equation (18) should represent the local criterion for squelching axisymmetric exponentially growing modes (ref. 16). Therefore,

$$Q = \frac{\sigma_r}{\sigma_{r,min}}$$

is used as a parameter in investigating the stability of the disks. The value $Q = 1$ is expected to be a lower bound on the rms velocities needed for stability. Using $f(r,v_r,v_\theta)$ as given by equation (21) results in (since v_r and $v_\theta - r\omega$ appear in the same form in equation (21), $\sigma_\theta^2 = \sigma_r^2$)

$$\sigma_\theta^2 + \sigma_r^2 = 2\sigma_r^2$$

$$= \frac{1}{\mu(r)} \iint \left[v_r^2 + (v_\theta - r\omega)^2\right] f(r,v_r,v_\theta) dv_r\, dv_\theta$$

$$= \frac{2}{3}(\omega_o^2 - \omega^2)(R^2 - r^2)$$

or

$$\sigma_r = \left[\frac{(\omega_o^2 - \omega^2)(R^2 - r^2)}{3}\right]^{1/2} \tag{22}$$

For the uniformly rotating disk, $\sigma_{r,min}$ is given by equation (5), so that

$$Q = \frac{\sigma_r}{\sigma_{r,min}} = 1.69\sqrt{1 - (\omega/\omega_o)^2} \tag{23}$$

The variation of Q as a function of ω for the uniformly rotating disk is shown in figure 24. The value of Q varies from zero for $\omega = \omega_o$ to 1.69 for $\omega = 0$; Q is equal to 1 for $\omega \approx 0.8\omega_o$.

Results

The results presented in this section were obtained with a 128×128 active mesh for the potential calculations. The disks consisted of 100 000 stars and there were 200 time steps per rotation.

The case of a cold disk $\omega = \omega_0$ was previously investigated (ref. 3) and as expected the disk was found to be violently unstable. The present investigation considers disks with $\omega = 0.8\omega_0$, $\omega = 0.6\omega_0$, $\omega = 0.4\omega_0$, and $\omega = 0$ corresponding to initial values of Q given by $Q = 1.01$, $Q = 1.35$, $Q = 1.55$, and $Q = 1.69$, respectively, where Q is given by equation (23). It should be emphasized that the model galaxies represented by equation (21) do not represent a mass or velocity distribution that one would expect to find in nature. For example, for the maximum velocity at a given radius

$$V_{max} = \sqrt{(\omega_0^2 - \omega^2)(R^2 - r^2)}$$

$f(r,v_r,v_\theta)$ as given by equation (21) is actually singular, and $f(r,v_r,v_\theta)$ increases with increasing v_r or v_θ. However, presently there are no really "good" stationary solutions of the collisionless Boltzmann equation available for disk galaxies. Some interesting solutions for self-gravitating disklike stellar systems are discussed by Miyamoto (ref. 17).

The evolution of four disks of stars corresponding to equation (21) with (a) $\omega = 0.8\omega_0$, (b) $\omega = 0.6\omega_0$, (c) $\omega = 0.4\omega_0$, and (d) $\omega = 0$ is presented in figure 25. Each of the 100 000 stars in the simulation represents 0.84×10^6 solar masses, so that the total mass of the disk galaxy is $0.84 \times 10^{11} M_\odot$ (solar masses). The rectangular border enclosing the disks represents the active 128×128 array of cells used in the calculations. The initial radius of the disks is 16 kpc. Since the disks become progressively more stable as the initial velocity dispersion is increased (or ω is decreased), the evolution of the more stable systems is investigated for longer times. The times shown in figure 25 and subsequent figures are in units of the rotational period of the cold (zero-velocity-dispersion) disk $T_0 = 2\pi/\omega_0$. Figure 25(a) shows that for $Q = 1$ (or $\omega = 0.8\omega_0$), the system is unstable and within two rotations it has formed a bar-shaped structure. After three rotations this structure remains essentially unchanged. It should be noted that all small-scale instabilities which occurred in the cold disk (ref. 3) have been stabilized. Only the large-scale "bar making" instability is present. A similar result is shown in figure 25(b) for $Q = 1.35$, or $\omega = 0.6\omega_0$. However, the bar structure is now much less pronounced. For $Q = 1.55$, the system is essentially stable. Some of the stars near the edge of the disk tend to escape to larger radii. This is to be expected since the distribution function $f(r,v_r,v_\theta)$ is singular at the edge and star orbits tend to be unstable there. Similar results are obtained for the nonrotating disk shown in figure 25(d). Figure 25 indicates that the disk becomes stable for values of Q somewhere

between 1.35 and 1.55, or for values of ω between $0.6\omega_0$ and $0.4\omega_0$. These results are in agreement with a normal-mode analysis of a family of uniformly rotating disks which was performed by Agris J. Kalnajs at Tel-Aviv University, Tel-Aviv, Israel. In his analysis (as yet unpublished), Kalnajs finds that the simple mode corresponding to the bar disturbance becomes unstable for values of ω greater than about 0.508.

The evolution of the distribution of the radial velocities of the stars as a function of star radial distance is shown in figure 26. As can be seen from figures 26(a) and (b), the radial velocities of the stars increase rapidly as the system evolves. Also, a large number of stars greatly increase their distance from the center of the disk. For $\omega = 0.4\omega_0$ and $\omega = 0$, the results in figures 26(c) and (d) show that there is little increase in the radial velocities, which of course were already large at $t = 0$. Only a few stars increase their radial distance beyond the initial disk radius, especially for the disk in figure 26(d). Nevertheless, the distribution of radial velocities at $t = 3$ in figure 26(d) shows that quite subtle changes take place in the velocity distribution near the edge of the disk. However, these changes do not appear to affect the structure of the disk appreciably. The rectangular border enclosing the velocity distributions in figure 26 extends from -350 km/sec to 350 km/sec and from 0 to 30 kpc.

In order to obtain more quantitative information than can be obtained from figures 25 and 26, the disk is divided into a number of concentric rings, each 1/2 kpc in width. The radial dependence of various parameters averaged azimuthally over each ring is then obtained.

An indication of how hot a disk of stars becomes can be obtained from the evolution of $Q = \frac{\sigma_r}{\sigma_{r,min}}$. Figure 27 shows the evolution of the azimuthally averaged Q for the four disks. The results in figure 27(a) indicate that the disk becomes rather hot, with values of Q in the outer parts of the disk near 5. For the disk with an initial angular velocity of $\omega = 0.6\omega_0$, the value of Q increases from 1.35 to about 2. Smaller increases occur for the disk in figure 27(c). Finally, the value of Q in figure 27(d) for the nonrotating disk remains nearly constant at 1.69.

The evolution of the azimuthally averaged density for the four disks is presented in figure 28. For the most unstable disk, shown in figure 28(a), the final central density increases to a high value given by an approximately exponential density variation. Similar results were previously obtained for other violently unstable disk galaxies (ref. 3). In figure 28(b) the central density oscillates between 1.4×10^8 and 2.1×10^8 $M_\odot/kpc^2$, reaching a final value of about 1.7×10^8 $M_\odot/kpc^2$ after 4.5 rotations. The changes in the density for the disk shown in figure 28(c) were the least pronounced of the four disks. For the nonrotating disk in figure 28(d) the central density appears to be oscillating near the value 1.4×10^9 $M_\odot/kpc^2$. When the kinetic energy of the disks is plotted as a function

of time, it is found that the kinetic energy initially oscillates nearly sinusoidally about the equilibrium value. The initial amplitude of the oscillations is about 5 percent of the equilibrium value and the period of the oscillations in all four cases is near (slightly less than) the rotational period of the cold balanced disk. For the disks in figures 25(a) and (b), the oscillations are strongly damped after the first two oscillations. For the disk in figure 25(c), the oscillations are more slowly damped, whereas for the disk in figure 25(d), the oscillations in the kinetic energy show no damping during the nine rotations investigated.

CONCLUDING REMARKS

The results on the evolution of initially balanced disks show that a velocity dispersion given by Toomre's criterion will stabilize a disk against axisymmetric disturbances. Also, all fast-growing small-scale disturbances are stabilized. However, all such "stabilized" disks investigated were found to be unstable against more slowly growing large-scale nonaxisymmetric disturbances, and the system consequently assumed a two-arm spiral structure. After about three rotations, the spiral structure disappears and the central portion of the disks assumes an oval or bar-shaped structure surrounded by a hot axisymmetric distribution of stars. In addition to the results presented here, the evolution of disks for which the logarithm of the initial density decreased linearly and quadratically with radius (i.e., exponential or Gaussian laws) is also investigated. The results obtained were similar to those presented here.

It was possible to generate an axisymmetric stable disk only with considerable difficulty. The initial condition for the axisymmetric stable disk was obtained by symmetrizing out the bar or oval structure in the central portion of the disk. The resulting axisymmetric disk was stable, and the radial variations of all parameters remained as they were for the final state of the disk with the central bar structure.

Attempts at slow cooling of stable axisymmetric disks indicated that whenever $Q = \frac{\sigma_r}{\sigma_{r,min}}$ (the ratio of the velocity dispersion to the minimum velocity dispersion given by Toomre's stability criterion) reached about 2, further cooling would only cause the occurrence of collective instabilities which would heat up the disk as fast as it was being cooled.

An interesting end result for all the disks of stars (which evolved from an initially unstable state) investigated so far is that the final distribution in the radial direction for the "disk population of stars" is closely approximated by an exponential variation of density. This result may be significant since it agrees with observational evidence which indicates that the luminosity in the outer regions of many spiral and SO galaxies seems also to decrease exponentially with radius.

The attempt to induce spiral structure by means of the passage of a companion galaxy was only partly successful. Because of the rather large velocity dispersion of the disturbed galaxy the induced spiral structure was weak.

The investigation of a disk of stars which is a stationary solution of the collisionless Boltzmann equation showed that the disk became unstable at a value of the velocity dispersion which agreed with the predictions made by a normal-mode analysis. For rotational velocities ω of $0.8\omega_0$ and $0.6\omega_0$ (where ω_0 is the rotational velocity of the cold, zero-velocity-dispersion disk) corresponding to $Q = 1$ and 1.35, respectively, the disk formed a barlike structure. For $\omega = 0.4\omega_0$ and $\omega = 0$ (or $Q = 1.55$ and $Q = 1.69$), the disk was stable against the bar-forming mode; however, for these two cases the disks sustained what appear to be natural oscillations, or pulsations, with a period near the rotational period of the cold balanced disk. The pulsations were especially pronounced for the nonrotating disk, where they did not show a decrease in amplitude for the nine rotations investigated. Since the initial conditions were generated by means of a pseudorandom-number generator, small oscillations are to be expected.

Langley Research Center,
National Aeronautics and Space Administration,
Hampton, Va., February 10, 1972.

APPENDIX

COMPUTER MODEL

Discretization Parameters

The model for the disk galaxy consists of a large number of representative stars (here 100 000) that are confined to move in the galactic disk. An $N \times N$ (here 256×256) array of cells is superposed over the plane of the disk for the purpose of calculating the gravitational potential. At the center of each cell a mass density is defined which is given by the number of stars in that cell. The mass-density distribution is used to obtain the gravitational field at the center of each cell. From the gravitational field the force acting at the position of a star is calculated by means of a bilinear interpolation among the fields of the four cell centers surrounding the star. Newton's equations of motion are then used to advance the position and velocity of each star by a small time step. Typically, there are 200 time steps per "galactic rotation." If a star should leave the $N \times N$ array of cells, it is still included in the calculations by approximating the force acting on the star. With the exception of the improved potential solver described in this appendix, the model used is the same as that previously described (ref. 3).

The effects of varying the number of stars and various other discretization parameters were investigated by Hohl and Hockney (ref. 2). The effect of binary collisions for the model has been estimated (ref. 3) to be such that the collision time equals about 100 "galactic rotations." The time history of the velocity dispersion of stars near various radii presented in figure 14 also indicates that collisional or thermalization effects are unimportant for the time period used for the present calculations.

Potential Calculation

The scaled gravitational potential at the center of cell (x,y) is defined by the double summation over the two-dimensional array of cells

$$\phi_{x,y} = \sum_{i=0}^{N-1} \sum_{j=0}^{N-1} \mu_{i,j} H_{i-x,j-y} \tag{A1}$$

where

$$H_{i,j} = \left(i^2 + j^2\right)^{-1/2} \qquad (i + j \neq 0)$$

$$H_{0,0} = 1$$

and $\mu_{i,j}$ is the mass density in cell (i,j). The double summation is evaluated by the convolution method using fast Fourier transforms (ref. 2). That is, the Fourier transform of the potential equals the product of the Fourier transforms of μ and H

$$\tilde{\phi}_{k,\ell} = \tilde{\mu}_{k,\ell}\tilde{H}_{k,\ell} \tag{A2}$$

The gravitational potential $\phi_{x,y}$ is obtained by taking the inverse Fourier transform of equation (A2). Rather than using a complex Fourier series, a real expansion was chosen. For example, the Fourier transform of the density $\mu_{x,y}$ is given by

$$\left.\begin{aligned}
\tilde{\mu}_{k,\ell} &= \sum_{y=0}^{N-1}\sum_{x=0}^{N-1} c(x)c(y)\mu_{x,y}\cos\left(\frac{\pi kx}{n}\right)\cos\left(\frac{\pi \ell y}{n}\right) && (0 \leqq k,\ \ell \leqq n)\\
\tilde{\mu}_{k,\ell} &= \sum_{y=0}^{N-1}\sum_{x=0}^{N-1} c(x)\mu_{x,y}\cos\left(\frac{\pi kx}{n}\right)\sin\left[\pi(\ell - n)\frac{y}{n}\right] && \begin{matrix}(0 \leqq k \leqq n)\\ (n < \ell < N)\end{matrix}\\
\tilde{\mu}_{k,\ell} &= \sum_{y=0}^{N-1}\sum_{x=0}^{N-1} c(y)\mu_{x,y}\sin\left[\pi(k - n)\frac{x}{n}\right]\cos\left(\frac{\pi \ell y}{n}\right) && \begin{matrix}(n < k < N)\\ (0 \leqq \ell \leqq n)\end{matrix}\\
\mu_{k,\ell} &= \sum_{y=0}^{N-1}\sum_{x=0}^{N-1} \mu_{x,y}\sin\left[\pi(k - n)\frac{x}{n}\right]\sin\left[\pi(\ell - n)\frac{y}{n}\right] && (n < k,\ \ell < N)
\end{aligned}\right\} \tag{A3}$$

where

$c(x) = 1/\sqrt{2}$ if $x = 0$ or $x = n$

$c(x) = 1$, otherwise

The symbol n defines the $n \times n$ active array and $N = 2n$ defines the larger array over which the Fourier transform must be taken so that the potential for an isolated disk galaxy is obtained. Note that the density may be nonzero only in the smaller $n \times n$ array. Because of the symmetry of $H_{x,y}$, the Fourier transform $\tilde{H}_{k,\ell}$ can be obtained by a finite cosine transform:

$$\tilde{H}_{k,l} = \sum_{y=0}^{n} \sum_{x=0}^{n} c^2(x)c^2(y)H_{x,y} \cos\left(\frac{\pi kx}{n}\right)\cos\left(\frac{\pi ly}{n}\right) \qquad (0 \leq k, \quad l \leq n) \qquad \text{(A4)}$$

and

$$\tilde{H}_{k+n,l} = \tilde{H}_{k,l+n} = \tilde{H}_{k+n,l+n} = \tilde{H}_{k,l}$$

The next step in obtaining the potential is to multiply $\tilde{\mu}_{k,l}$ by $\tilde{H}_{k,l}$ to obtain

$$\tilde{\phi}_{k,l} = \tilde{\mu}_{k,l}\tilde{H}_{k,l} \qquad \text{(A5)}$$

The gravitational potential for an isolated galaxy correctly defined over the $n \times n$ array is obtained by the Fourier synthesis

$$\phi_{x,y} = \frac{1}{N^2}\left(\sum_{l=0}^{n}\left\{\sum_{k=0}^{n} \tilde{\phi}_{k,l} \cos\left(\frac{\pi}{n} kx\right) + \sum_{k=n+1}^{N-1} \tilde{\phi}_{k,l} \sin\left[\frac{\pi}{n}(k - n)x\right]\right\}\cos\left(\frac{\pi}{n} ly\right)\right.$$

$$\left. + \sum_{l=n+1}^{N-1}\left\{\sum_{k=0}^{n} \tilde{\phi}_{k,l} \cos\left(\frac{\pi}{n} kx\right) + \sum_{k=n+1}^{N-1} \tilde{\phi}_{k,l} \sin\left[\frac{\pi}{n}(k - n)x\right]\right\}\sin\left[\frac{\pi}{n}(l - n)y\right]\right) \qquad \text{(A6)}$$

A FORTRAN listing of the computer program actually used to obtain the potential by use of an $N \times n$ array of cells is given on the following page. The variable I2A defines the size of the rectangular array used for the potential calculations. When the subroutine GETPHI is called, RHO(I,J) contains the mass density and GETPHI places the values of the corresponding gravitational potential in RHO(I,J). The subroutine FTRANS(I,I2B) was written by Hockney (ref. 18) and it performs a finite Fourier analysis or synthesis on the COMMON input array Z and places the result in the COMMON output array Y. The subroutine performs a cosine analysis for I = 2, a periodic analysis for I = 3, and a periodic synthesis for I = 4. The subroutine GETSET(I,I2B) initializes FTRANS and is called every time the arguments of FTRANS(I,I2B) are changed. The Fourier transform $H_{k,l}$ is calculated on an (n+1) × (n+1) array only the first time that the subroutine is called and is kept in storage for subsequent use.

APPENDIX – Continued

SUBROUTINE FOR CALCULATING THE GRAVITATIONAL POTENTIAL

```
      SUBROUTINE GETPHI
      COMMON Z(257),Y(257),RHO(256,128),I2A,ITEST
      DIMENSION H(129,129)
      IF(ITEST.EQ.0) GO TO 10
      ITEST=0
      I2B=I2A-1
      N=2**I2A
      NO2=N/2
      N21=NO2+1
      RNI=1./(N*N)
      DO 1 J=1,N21
      DO 1 I=1,N21
      IF(I.EQ.1.AND.J.EQ.1) GO TO 1
      H(I,J)=RNI/SQRT((I-1.)*(I-1.)+(J-1.)*(J-1.))
    1 CONTINUE
      H(1,1)=RNI
      CALL GETSET(2,I2B)
      DO 2 J=1,N21
      DO 3 I=1,N21
    3 Z(I)=H(I,J)
      CALL FTRANS(2,I2B)
      DO 4 I=1,N21
    4 H(I,J)=Y(I)
    2 CONTINUE
      DO 5 I=1,N21
      DO 6 J=1,N21
    6 Z(J)=H(I,J)
      CALL  FTRANS(2,I2B)
      DO 7 J=1,N21
    7 H(I,J)=Y(J)
    5 CONTINUE
   10 CONTINUE
      CALL GETSET(3,I2A)
      DO 11 J=1,NO2
      DO  8 I=1,N
    8 Z(I)=RHO(I,J)
      CALL FTRANS(3,I2A)
      DO 9 I=1,N
    9 RHO(I,J)=Y(I)
   11 CONTINUE
      DO 12 I=1,N
      DO 13 J=1,NO2
      Z(J)=RHO(I,J)
   13 Z(J+NO2)=0.
      CALL GETSET(3,I2A)
      CALL FTRANS(3,I2A)
      IF(I.GT.N21) GO TO 14
      DO 15 J=2,NO2
      Z(J)=Y(J)*H(I,J)
   15 Z(J+NO2)=Y(J+NO2)*H(I,J)
      Z(1)=Y(1)*H(I,1)
      Z(N21)=Y(N21)*H(I,N21)
      GO TO 16
   14 DO 17 J=2,NO2
      Z(J)=Y(J)*H(I-NO2,J)
   17 Z(J+NO2)=Y(J+NO2)*H(I-NO2,J)
      Z(1)=Y(1)*H(I-NO2,1)
      Z(N21)=Y(N21)*H(I-NO2,N21)
   16 CONTINUE
      CALL GETSET(4,I2A)
      CALL FTRANS(4,I2A)
      DO 18 J=1,NO2
   18 RHO(I,J)=Y(J)
   12 CONTINUE
      DO 19 J=1,NO2
      DO 20 I=1,N
   20 Z(I)=RHO(I,J)
      CALL FTRANS(4,I2A)
      DO 21 I=1,N21
   21 RHO(I,J)=Y(I)
   19 CONTINUE
      RETURN
      END
```

Next the Fourier transform of $\mu_{x,y}$ in the x-direction is obtained on the $N \times n$ array, that is, for $0 \leq x \leq N - 1$ and $0 \leq y \leq n$. Since $\mu_{x,y}$ is nonzero only over the $n \times n$ array, the components of the Fourier transform of $\mu_{x,y}$ in the x-direction will be zero for $n < y < N$. Therefore, by use of the one-dimensional arrays Y and Z, one can perform the Fourier transform in the y-direction, multiply the result by $\tilde{H}_{k,\ell}$, and take the inverse Fourier transform in the y-direction. The result is placed in the $N \times n$ RHO(I,J) array for $0 \leq y \leq n - 1$ and $0 \leq x \leq N - 1$ with the values for $n < y < N$ discarded. The final step is to perform the inverse Fourier transform in the x-direction for $0 \leq y \leq n - 1$. This procedure gives the correct gravitational potential for an isolated disk galaxy over the $n \times n$ array.

Table I gives the measured time for calculating the gravitational potential with the program listed above. Also shown are the times required for the previous potential solver which required a larger $N \times N$ array. A listing of that program is given in reference 3.

APPENDIX – Concluded

TABLE I.- COMPUTER TIME REQUIRED TO OBTAIN THE GRAVITATIONAL POTENTIAL

Active $n \times n$ mesh	CDC 6600 CPU time, sec, for –			
	Present potential solver using $2(n \times n)$ storage		Previous potential solver using $4(n \times n)$ storage	
	$\tilde{H}$ calculated	$\tilde{H}$ given	$\tilde{H}$ calculated	$\tilde{H}$ given
16×16	0.164	0.126	0.182	0.144
32×32	.618	.476	.660	.526
64×64	2.440	1.892	2.626	2.086
128×128	10.000	7.740	10.794	8.530

REFERENCES

1. Miller, R. H.; and Prendergast, K. H.: Stellar Dynamics in a Discrete Phase Space. Astrophys. J., vol. 151, no. 2, Feb. 1968, pp. 699-709.

2. Hohl, Frank; and Hockney, R. W.: A Computer Model of Disks of Stars. J. Comput. Phys., vol. 4, no. 3, Oct. 1969, pp. 306-324.

3. Hohl, Frank: Dynamical Evolution of Disk Galaxies. NASA TR R-343, 1970.

4. Hohl, F.: Computer Models of Spiral Structure. The Spiral Structure of Our Galaxy, W. Becker and G. Contopoulos, eds., Springer-Verlag New York Inc., 1970, pp. 368-372.

5. Miller, R. H.; Prendergast, K. H.; and Quirk, William J.: Numerical Experiments on Spiral Structure. Astrophys. J., vol. 161, no. 3, pt. 1, Sept. 1970, pp. 903-916.

6. Toomre, Alar: On the Gravitational Stability of a Disk of Stars. Astrophys. J., vol. 139, no. 4, May 15, 1964, pp. 1217-1238.

7. Hunter, C.: The Structure and Stability of Self-Gravitating Disks. Mon. Notic. Roy. Astron. Soc., vol. 126, no. 4, 1963, pp. 299-315.

8. Hunter, C.: Oscillations of Self-Gravitating Disks. Mon. Notic. Roy. Astron. Soc., vol. 129, no. 4, 1965, pp. 321-343.

9. Hockney, R. W.; and Hohl, Frank: Effects of Velocity Dispersion on the Evolution of a Disk of Stars. Astron. J., vol. 74, no. 9, Nov. 1969, pp. 1102-1104, 1119-1124.

10. Freeman, K. C.: On the Disks of Spiral and SO Galaxies. Astrophys. J., vol. 160, no. 3, pt. 1, June 1970, pp. 811-830.

11. Freeman, K. C.: Structure and Evolution of Barred Spiral Galaxies, III. Mon. Notic. Roy. Astron. Soc., vol. 134, no. 1, 1966, pp. 15-23.

12. Julian, William H.: Overstability of Thin Stellar Systems. Astrophys. J., vol. 155, no. 1, pt. 1, Jan. 1969, pp. 117-122.

13. Lin, C. C.; Yuan, C.; and Shu, Frank H.: On the Spiral Structure of Disk Galaxies – III. Comparison With Observations. Astrophys. J., vol. 155, no. 3, pt. 1, Mar. 1969, pp. 721-746.

14. Chandrasekhar, S.: Principles of Stellar Dynamics. Enlarged ed., Dover Publ., Inc., 1960.

15. Jeans, James H.: Astronomy and Cosmogony. Dover Publ., Inc., c.1961.

16. Kalnajs, Agris J.: Dynamics of Flat Galaxies. I. Astrophys. J., vol. 166, no. 2, pt. 1, June 1, 1971, pp. 275-293.

17. Miyamoto, Masanori: A Self-Gravitating Disk-Like Stellar System. Publ. Astron. Soc. Japan, vol. 23, no. 1, 1971, pp. 21-32.

18. Hockney, R. W.: The Potential Calculation and Some Applications. Methods in Computational Physics, Vol. 9 – Plasma Physics, Berni Alder; Sidney Fernbach; and Manuel Rotenberg, eds., Academic Press, 1970, pp. 135-211.

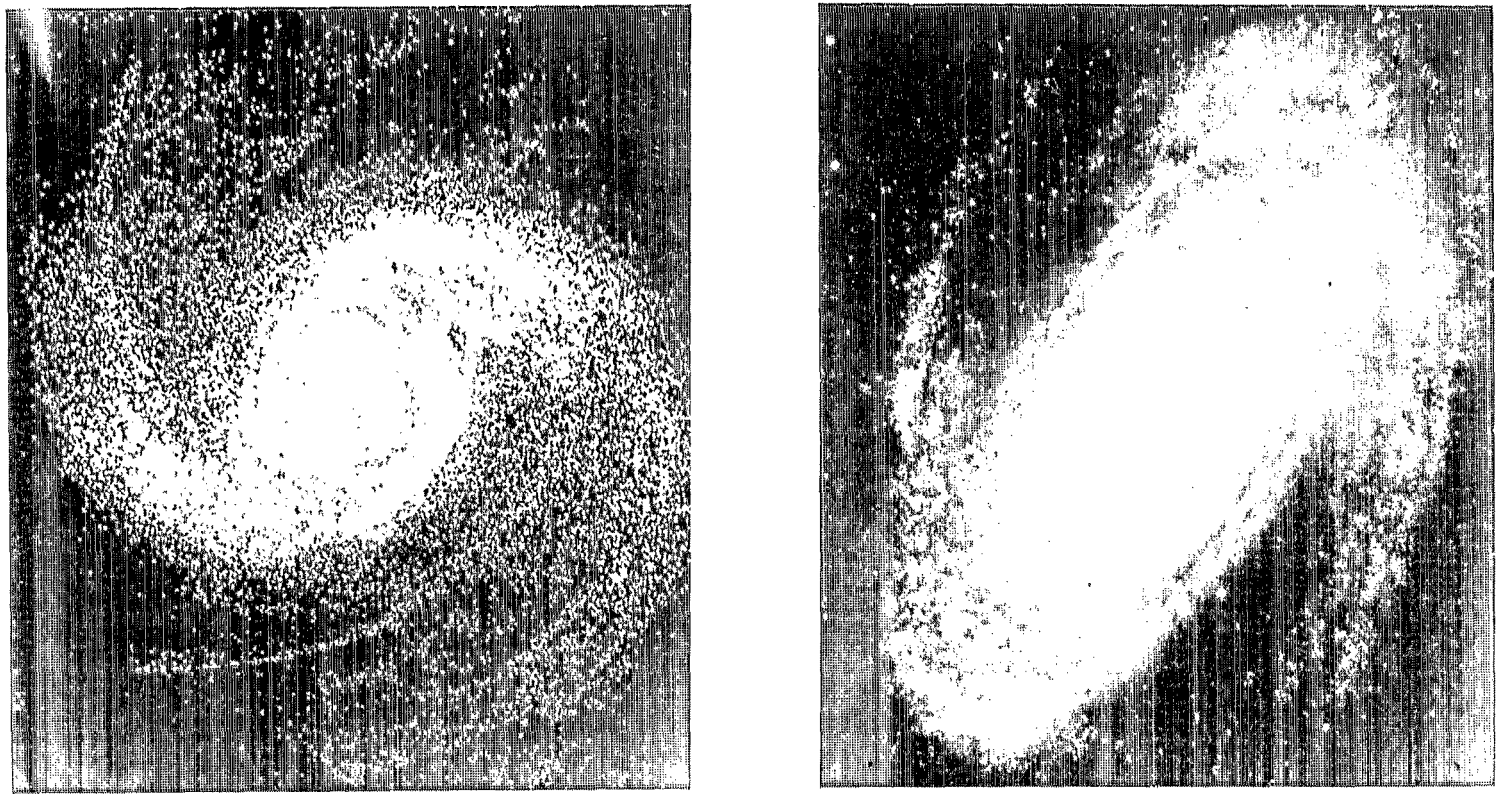

Computer simulation

M 81, Sb-type spiral galaxy

L-72-125

Figure 1.- Comparison of four computer-generated galaxies with photographs of actual galaxies.

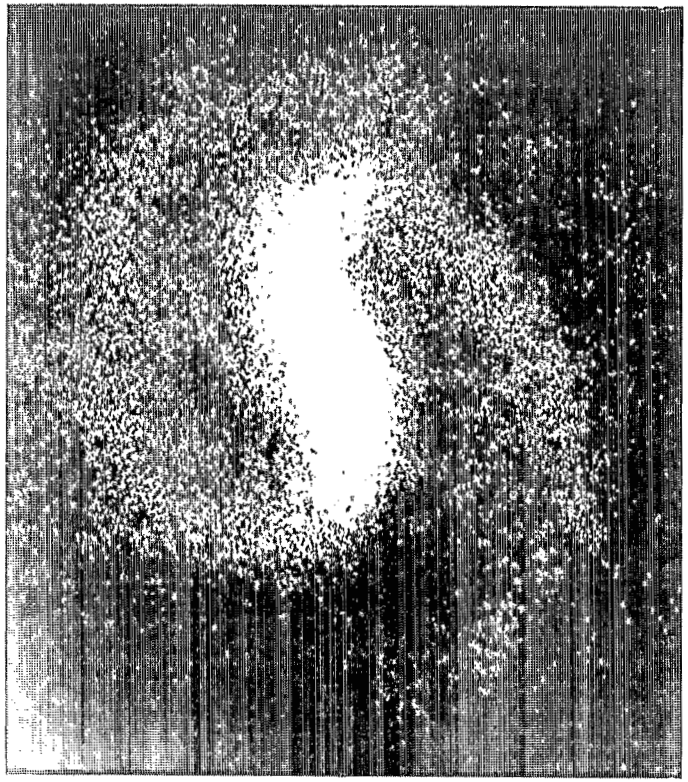

Computer simulation

NGC-175, SBab-type barred spiral galaxy

L-72-126

Figure 1.- Continued.

Computer simulation

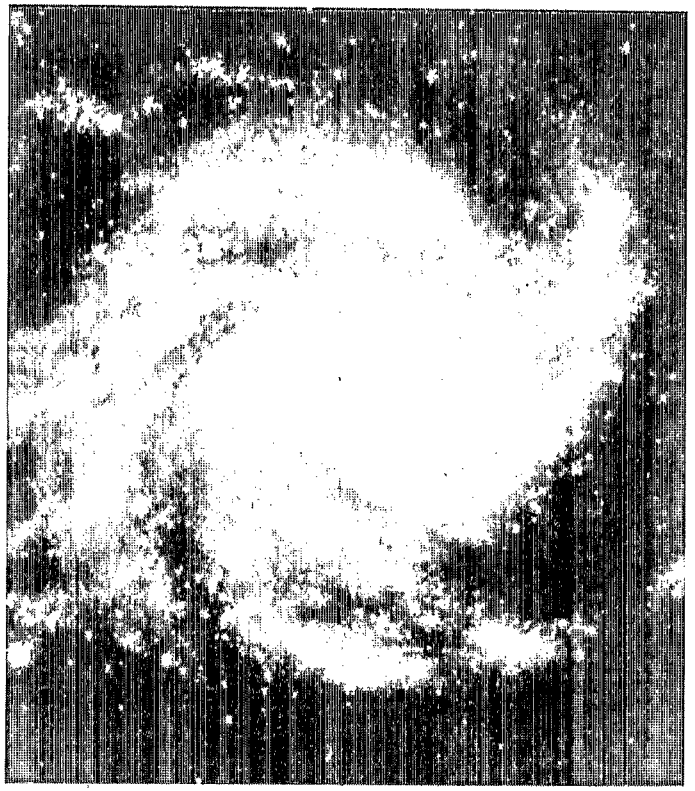

M 101, Sc-type regular spiral galaxy

L-72-127

Figure 1.- Continued.

Computer simulation

NGC-1073, SBc-type barred spiral galaxy

L-72-128

Figure 1.- Concluded.

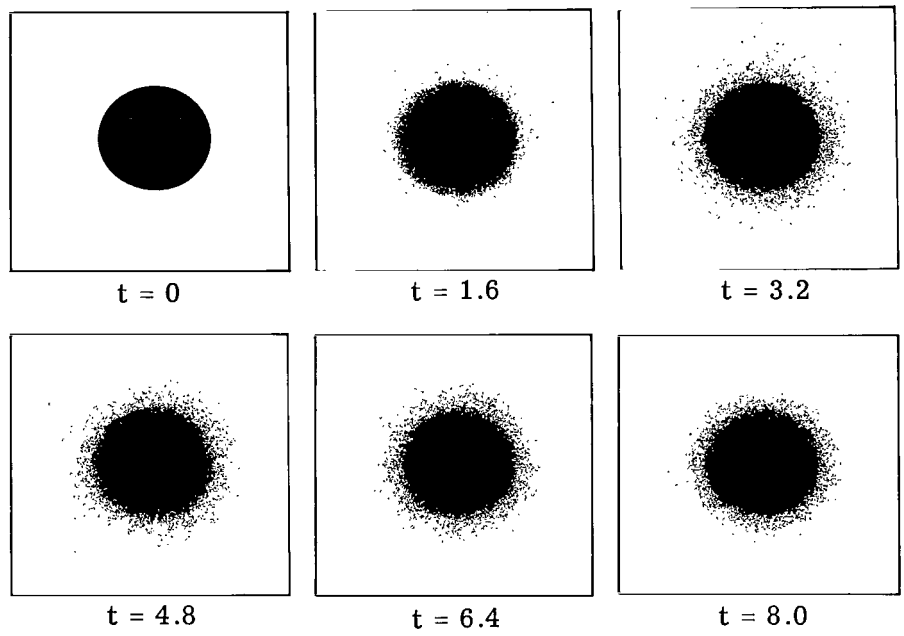

Figure 2.- Axisymmetric evolution of an initially balanced uniformly rotating disk of 100 000 stars. The stars have an initial velocity dispersion given by Toomre's criterion and move under a purely radial gravitational field. Time in this and all subsequent figures is given in units of the rotational period of the cold balanced disk.

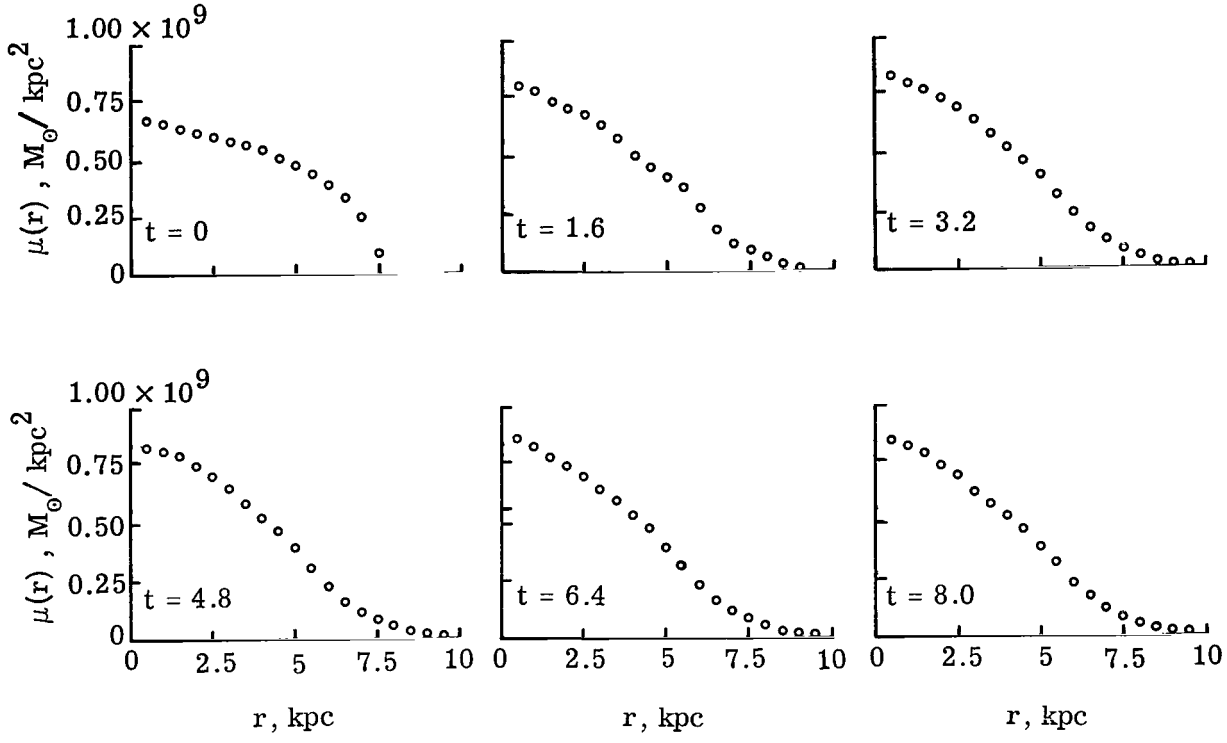

Figure 3.- Evolution of the density for the disk shown in figure 2.

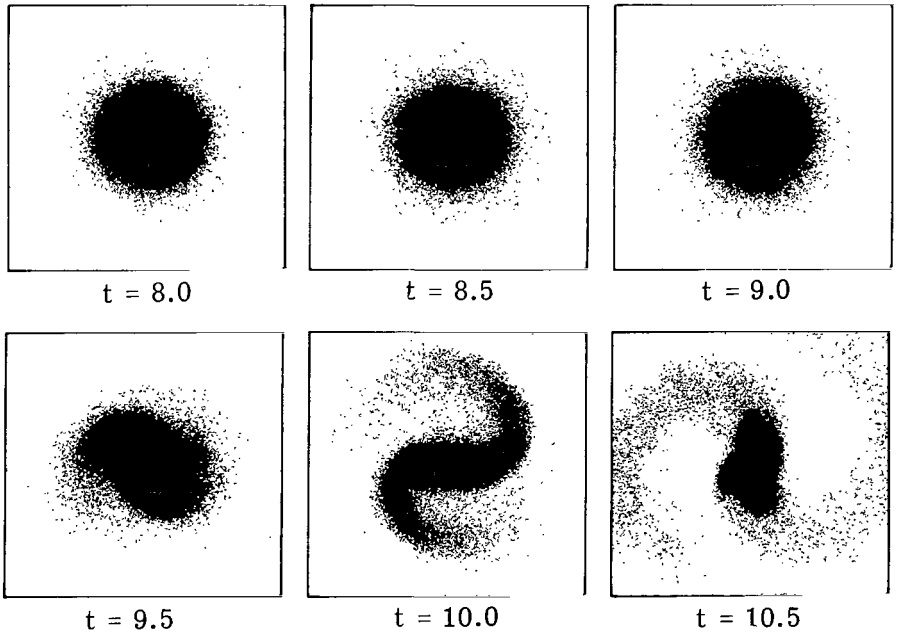

Figure 4.- Nonaxisymmetric evolution of the disk with an initial condition taken as the disk in figure 2 at t = 8.

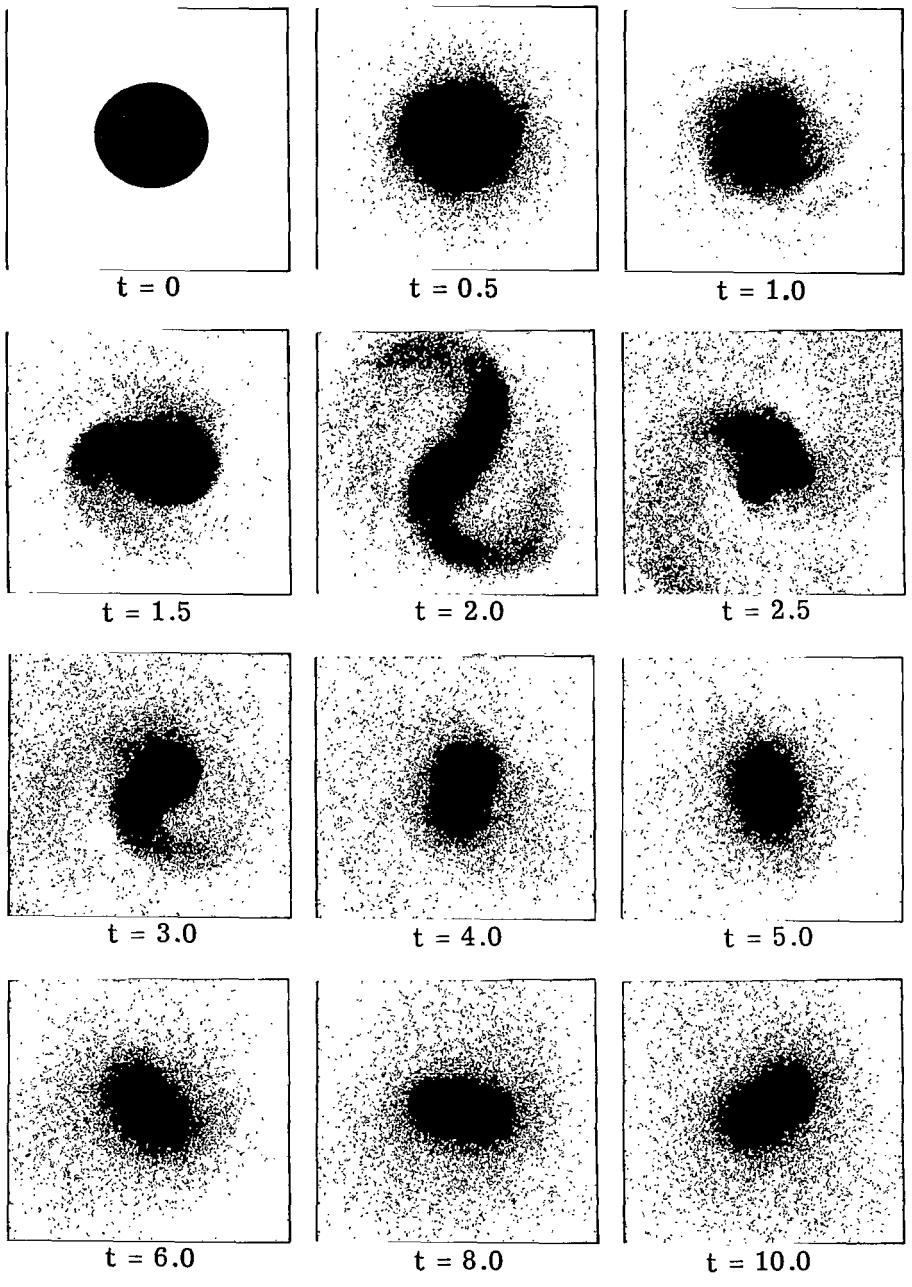

Figure 5.- Unconstrained evolution of the initially balanced uniformly rotating disk of 100 000 stars. The stars have an initial velocity dispersion given by Toomre's criterion.

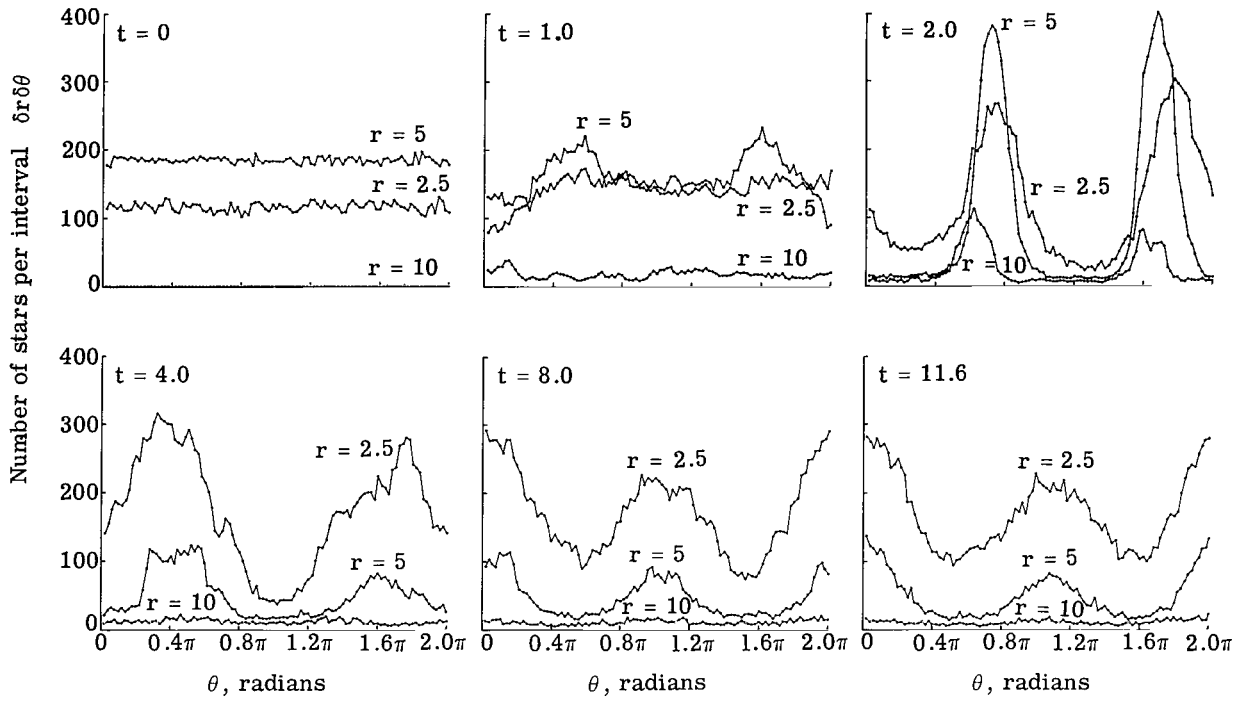

Figure 6.- Evolution of the azimuthal variation of the star density at three radii r (in kpc) for the disk shown in figure 5.

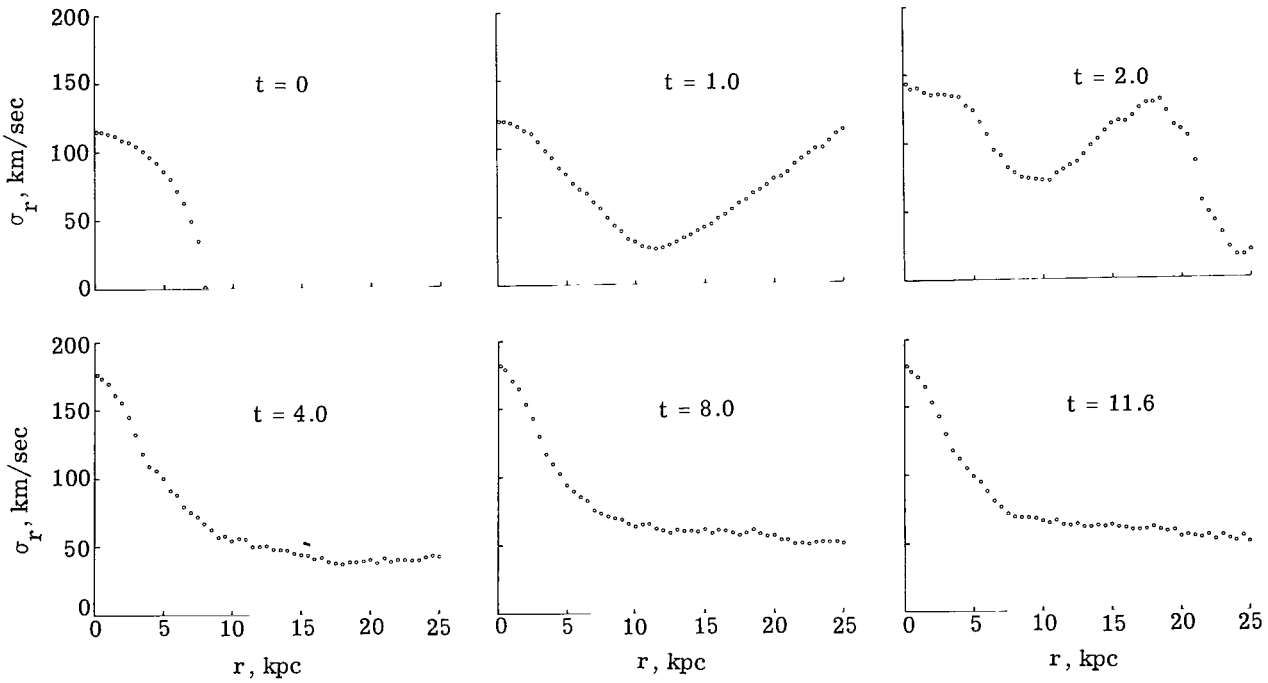

Figure 7.- Variation of the radial velocity dispersion as a function of radius for the disk shown in figure 5.

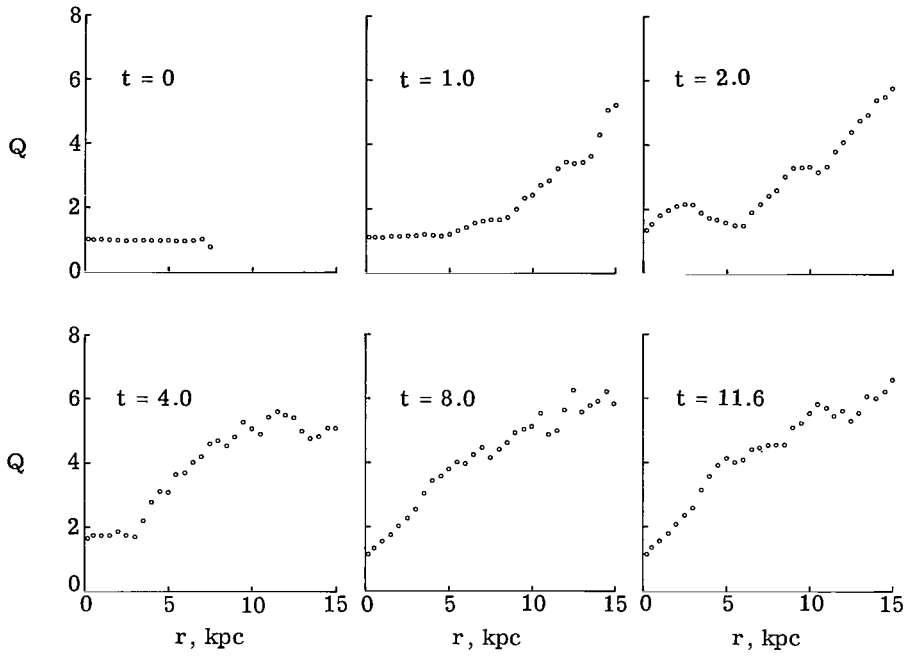

Figure 8.- Dependence of $Q = \sigma_r/\sigma_{r,min}$ on radius for the disk shown in figure 5.

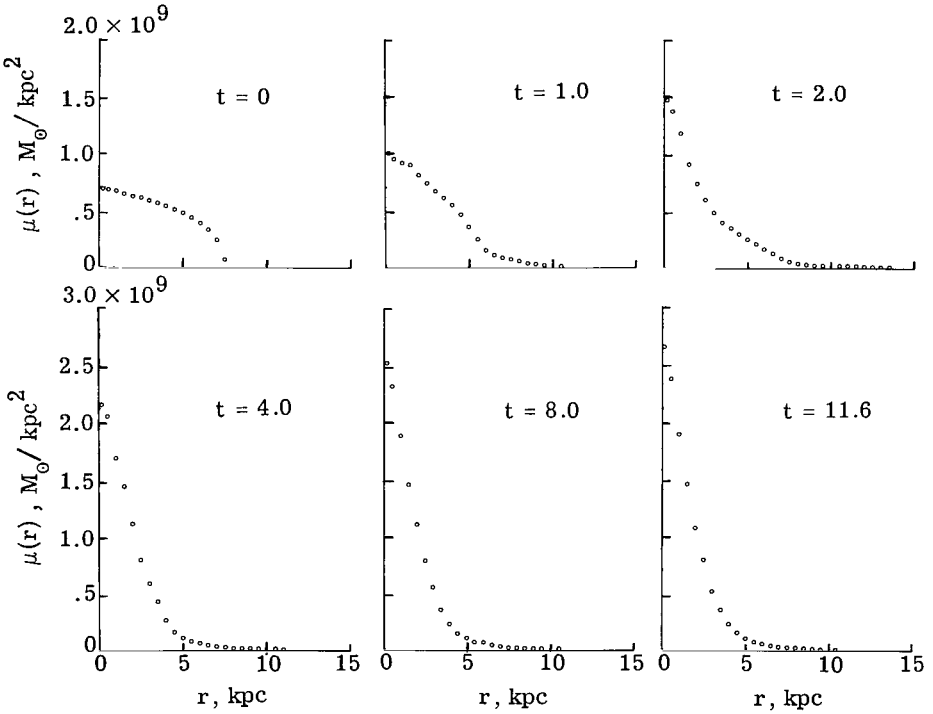

Figure 9.- Evolution of the mass density plotted as a function of radius. The density is given in units of solar masses per kpc^2. (Note that each one of the 100 000 simulation stars has a mass of $0.84 \times 10^6 M_\odot$.)

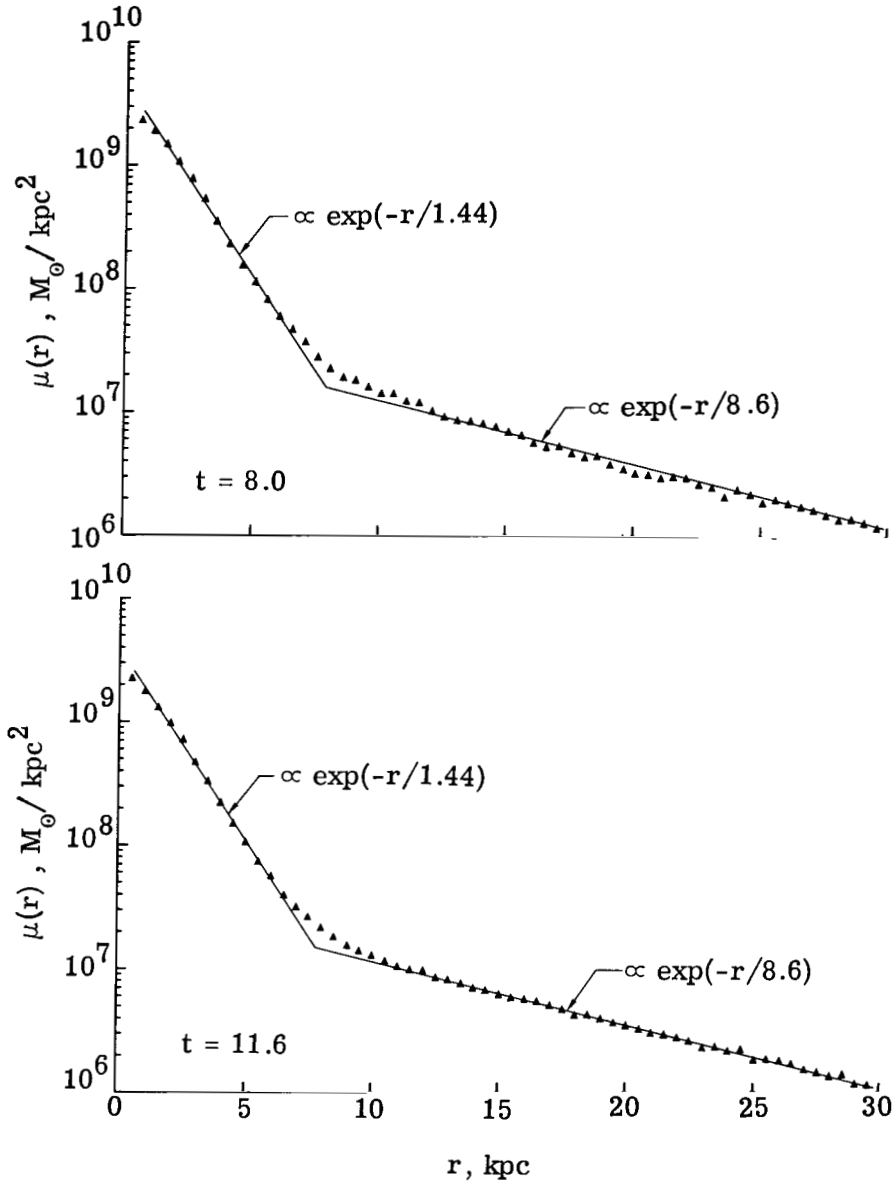

Figure 10.- Semilogarithmic plot of the density variation with radius after 8.0 and 11.6 rotations.

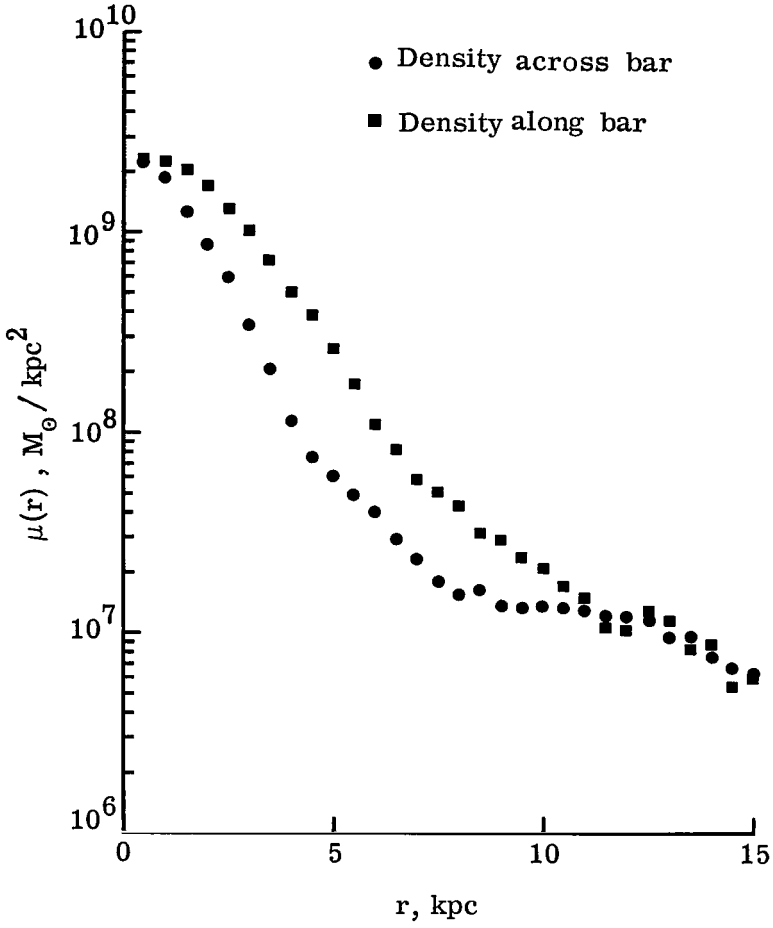

Figure 11.- Density variation along and across the bar at t = 8.0.

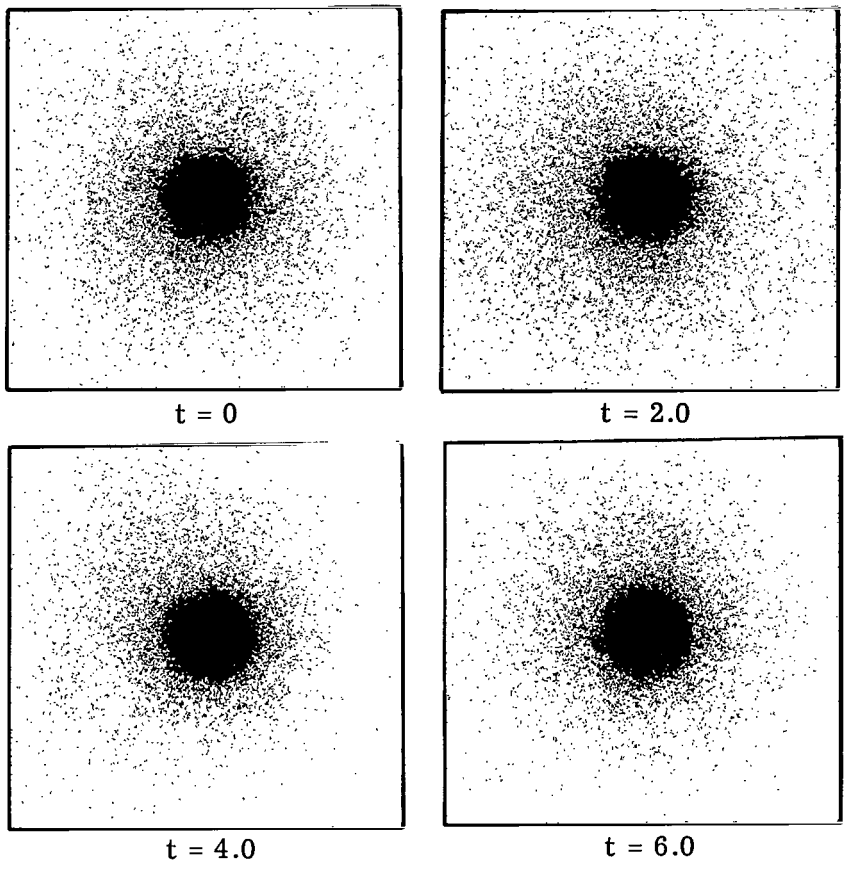

Figure 12.- Evolution of a stable axisymmetric disk of 100 000 stars. Time shown is in units of the rotational period of the cold balanced disk $T_o = \frac{2\pi}{\omega_o}$.

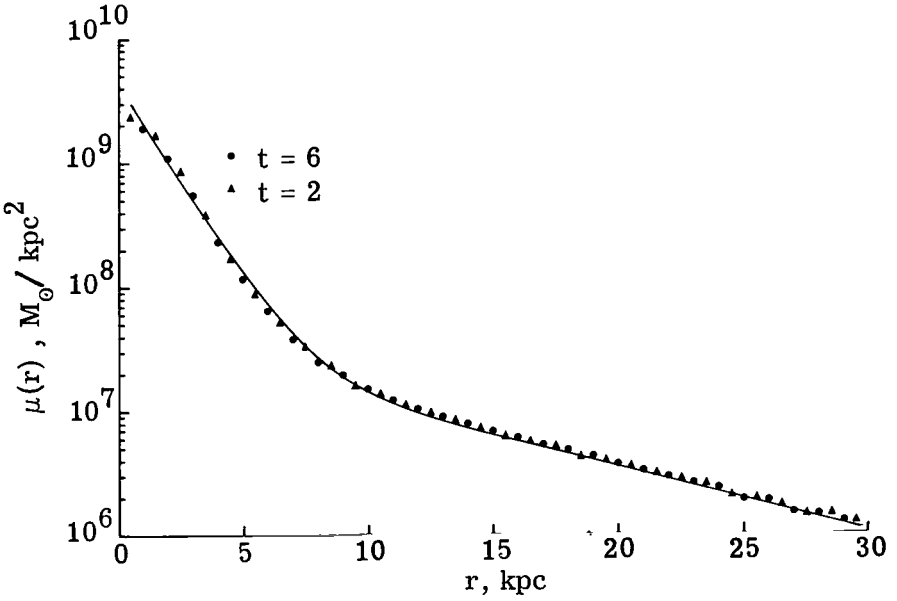

Figure 13.- Dependence of the density on radius for the stable axisymmetric disks after 2 and 6 rotations.

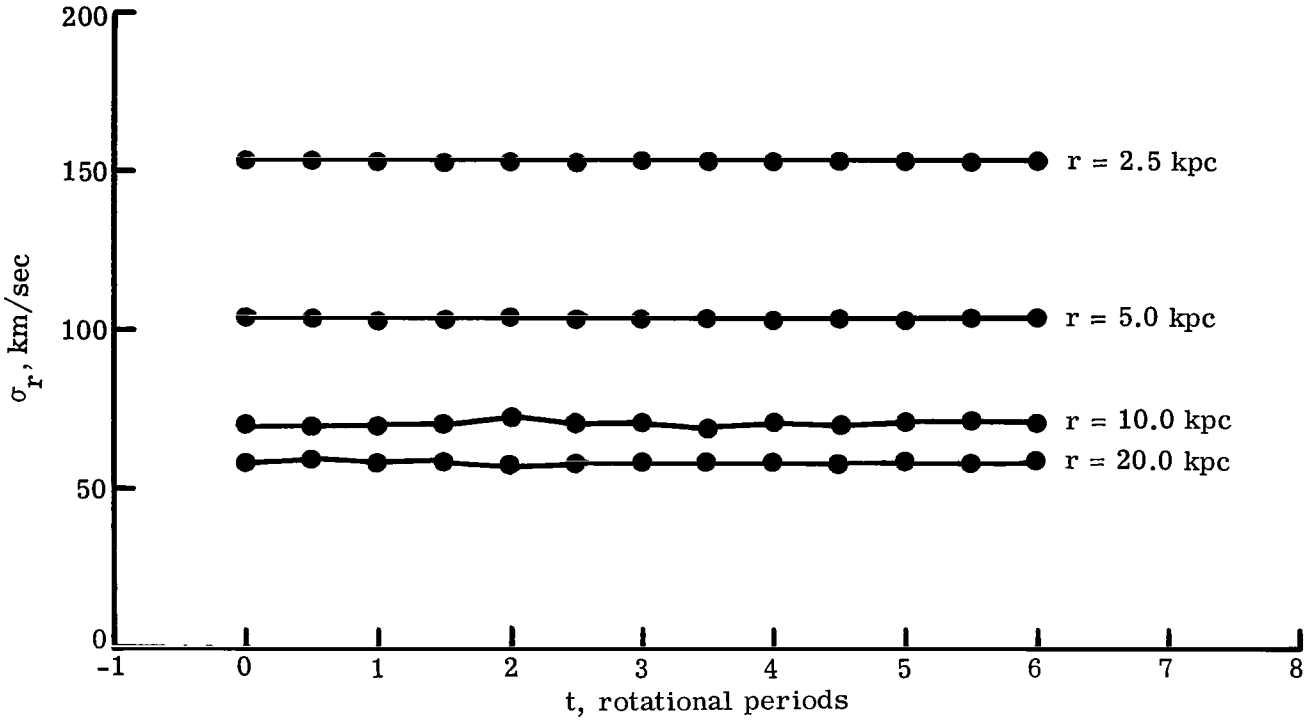

Figure 14.- Evolution in time of the rms velocity at four radii for the stable axisymmetric disk shown in figure 12.

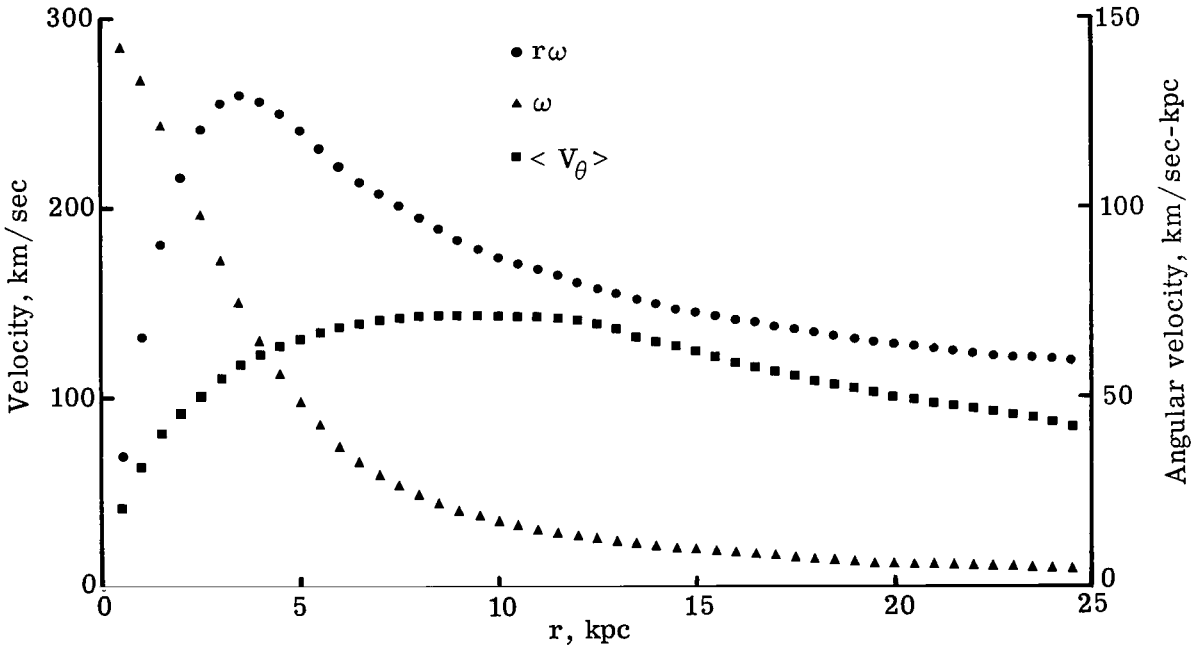

Figure 15.- Comparison of the radial variations of the angular velocity $\omega = \sqrt{K_r/r}$, the azimuthal velocity $r\omega$, and the mean azimuthal velocity of the stars $\langle V_\theta \rangle$.

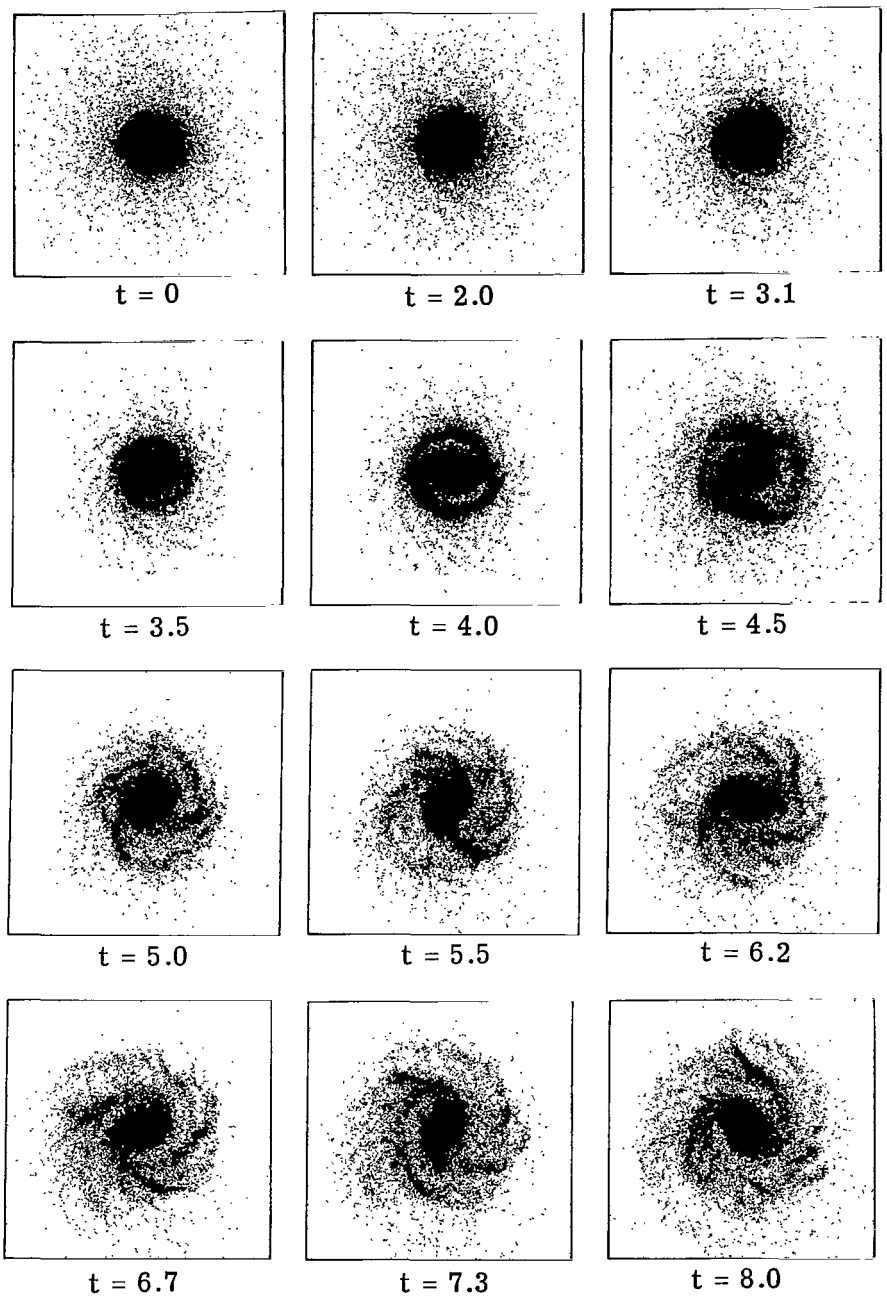

Figure 16.- Development of spiral structure for a galaxy for which per rotation 10% of the stars are placed in purely circular orbits.

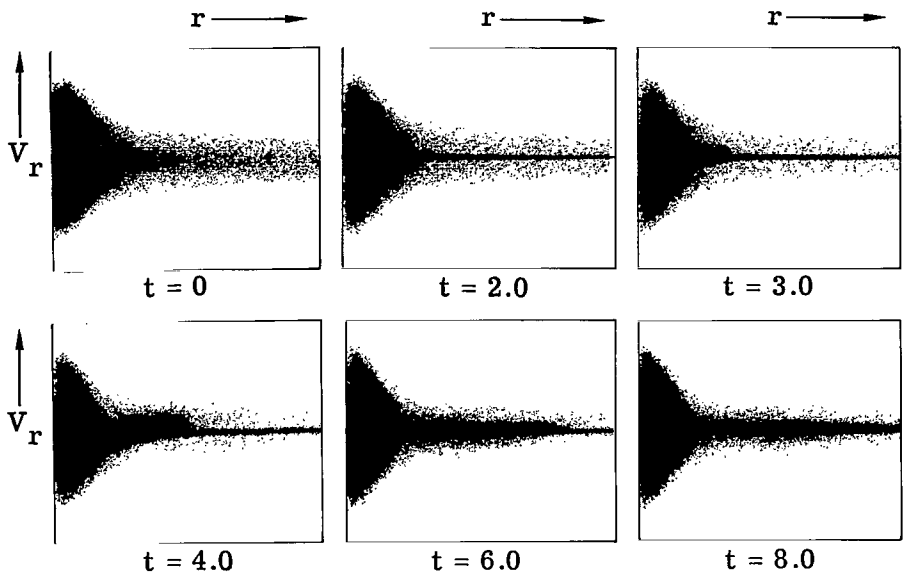

Figure 17.- Evolution of the radial velocities for the galaxy shown in figure 16.

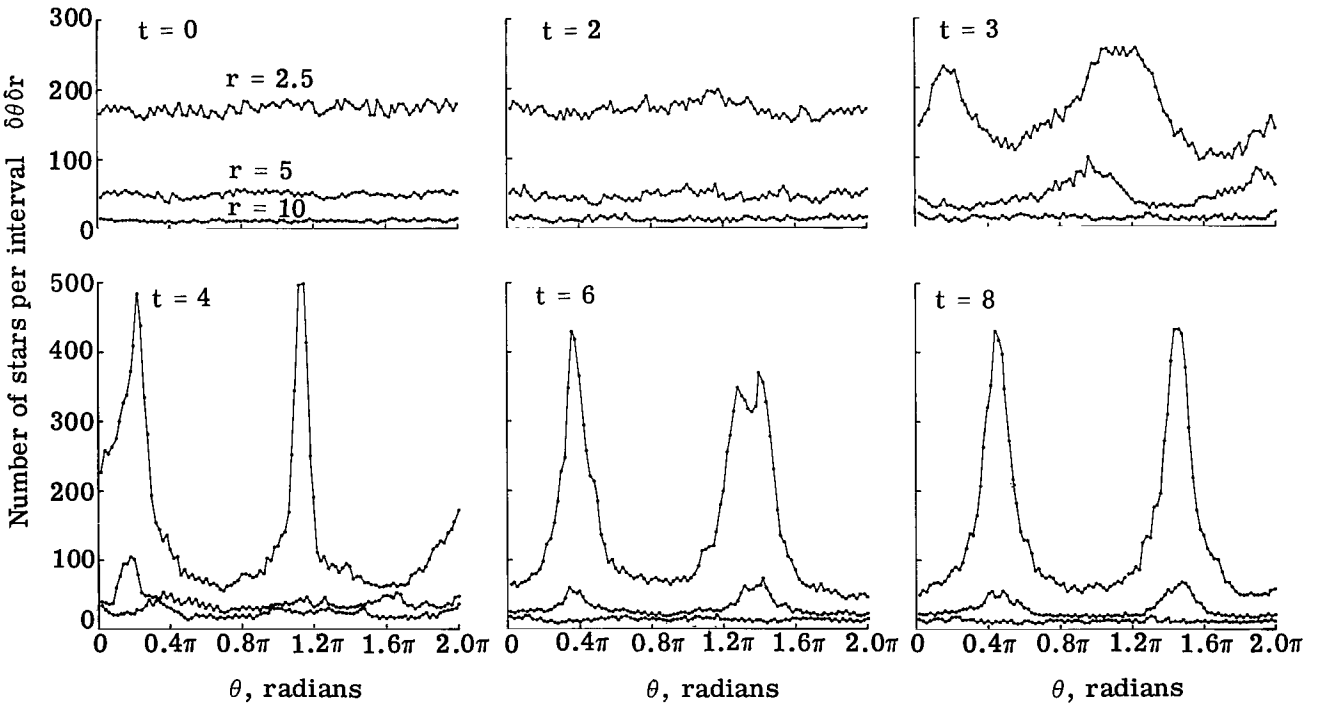

Figure 18.- Evolution of the azimuthal variation of the star number density at three radii for the disk shown in figure 16.

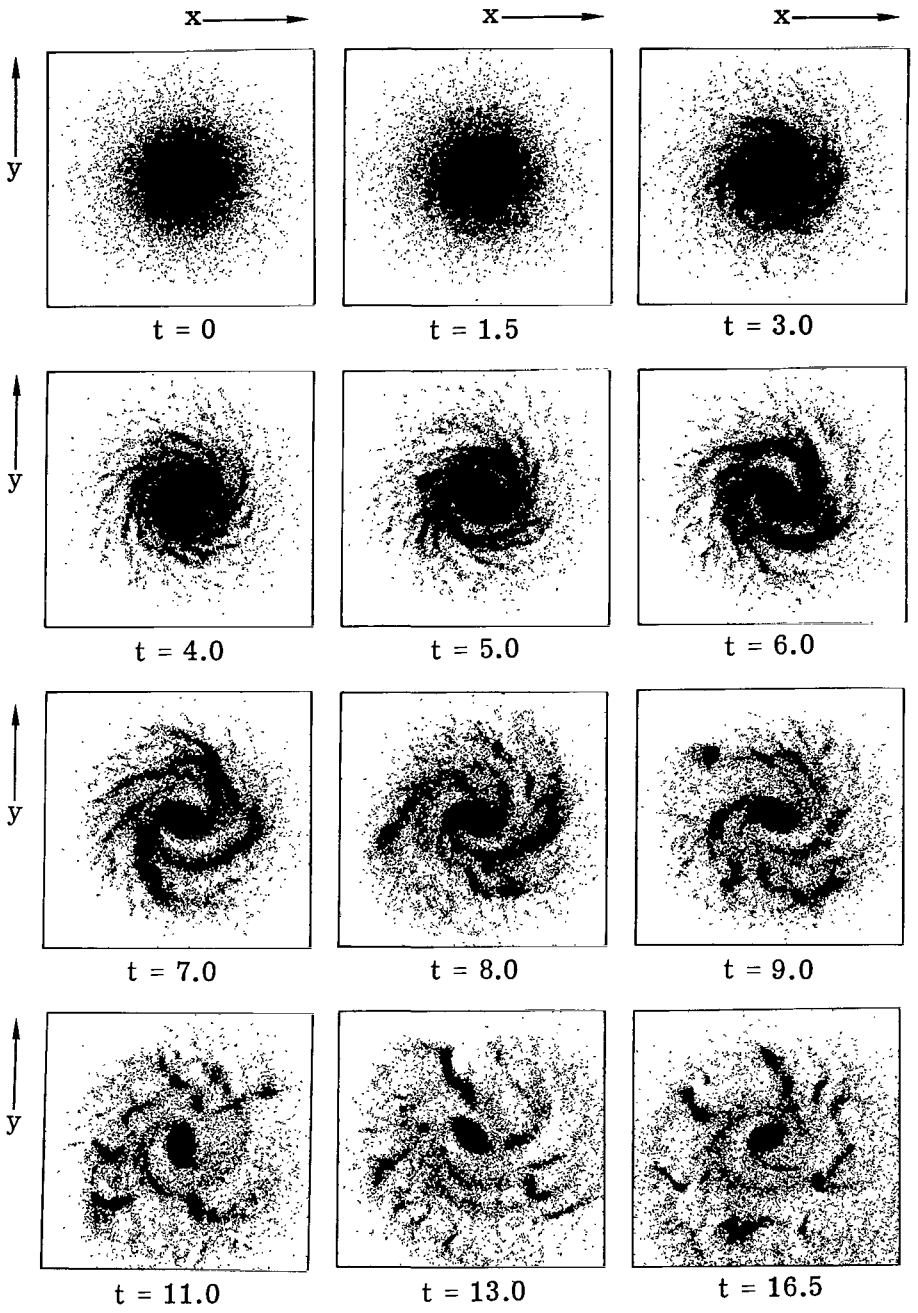

Figure 19.- Development of spiral structure and condensations for a galaxy where per rotation 30% of the stars have part of their random velocities removed.

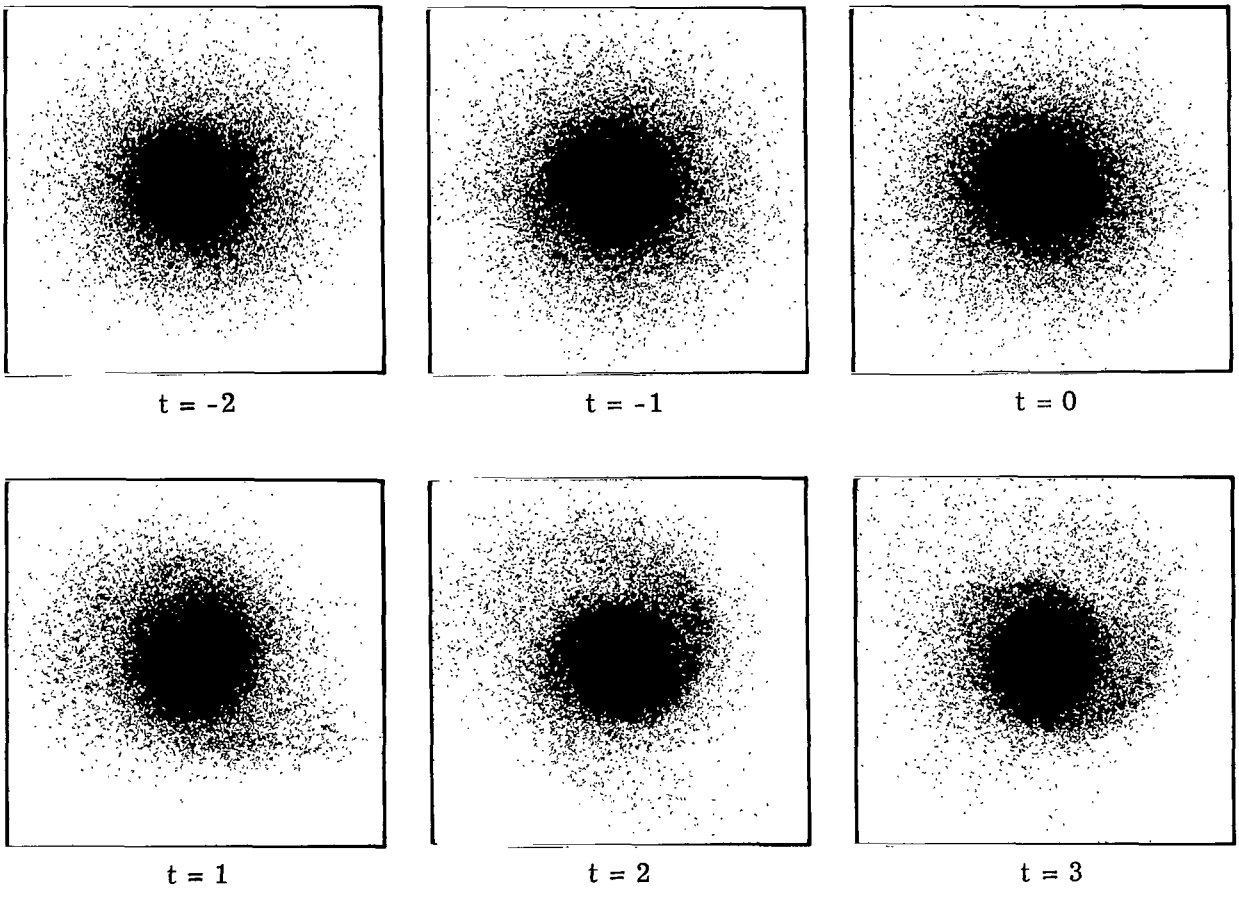

Figure 20.- Evolution of a galaxy under the influence of a companion galaxy.

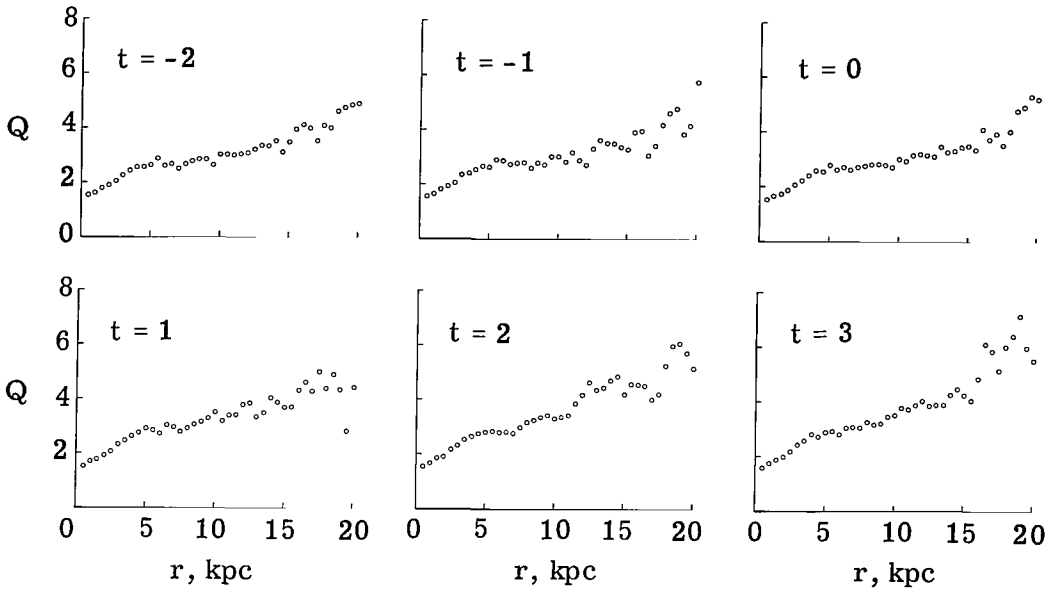

Figure 21.- Evolution of $Q = \sigma_r/\sigma_{r,min}$ for the galaxy shown in figure 20.

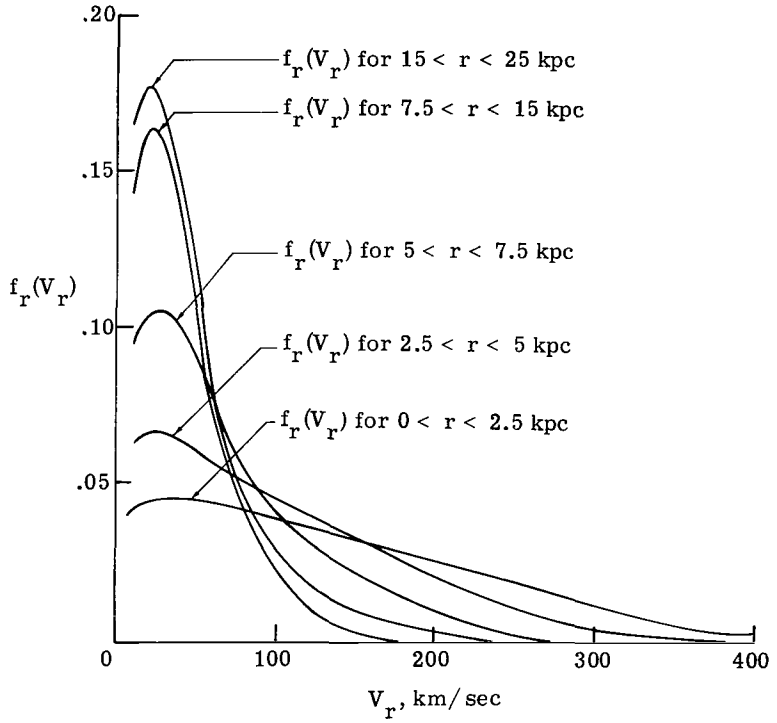

Figure 22.- Distribution of radial velocities for the galaxy shown in figure 20.

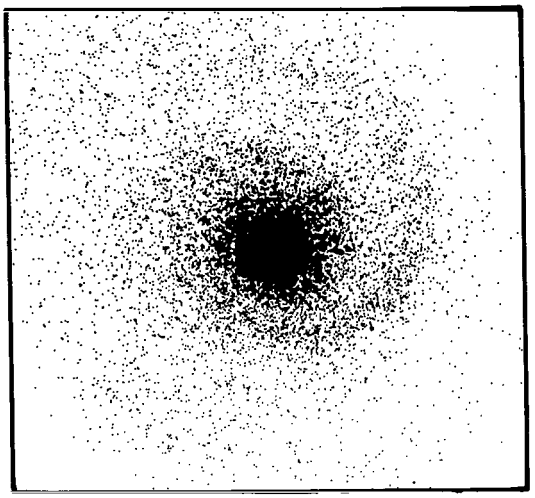

(a) $0 < V_r < 20.$

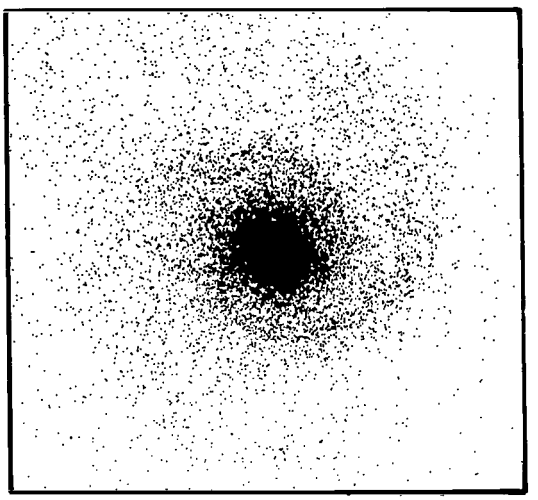

(b) $20 < V_r < 40.$

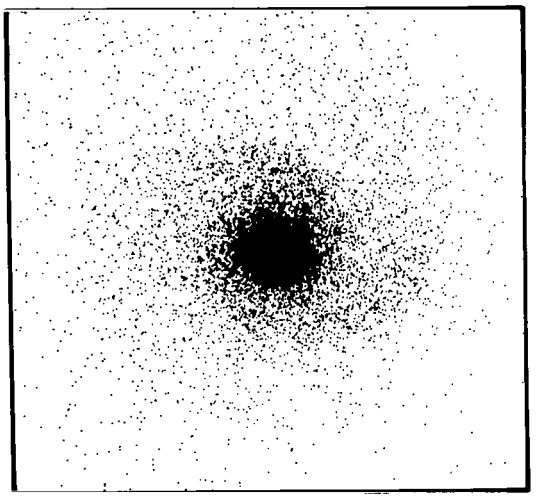

(c) $40 < V_r < 60.$

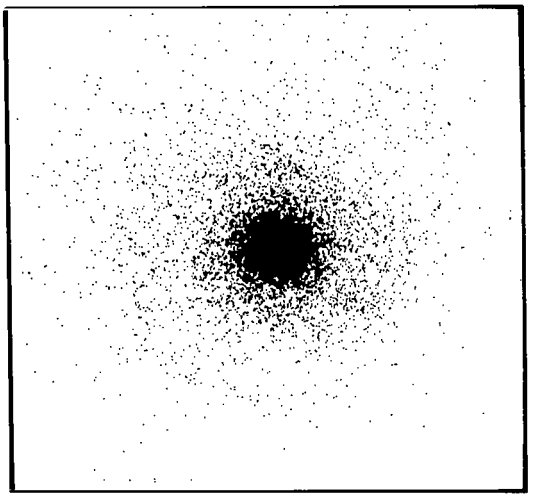

(d) $60 < V_r < 80.$

Figure 23.- Distribution of stars in four velocity intervals at $t = 3.$

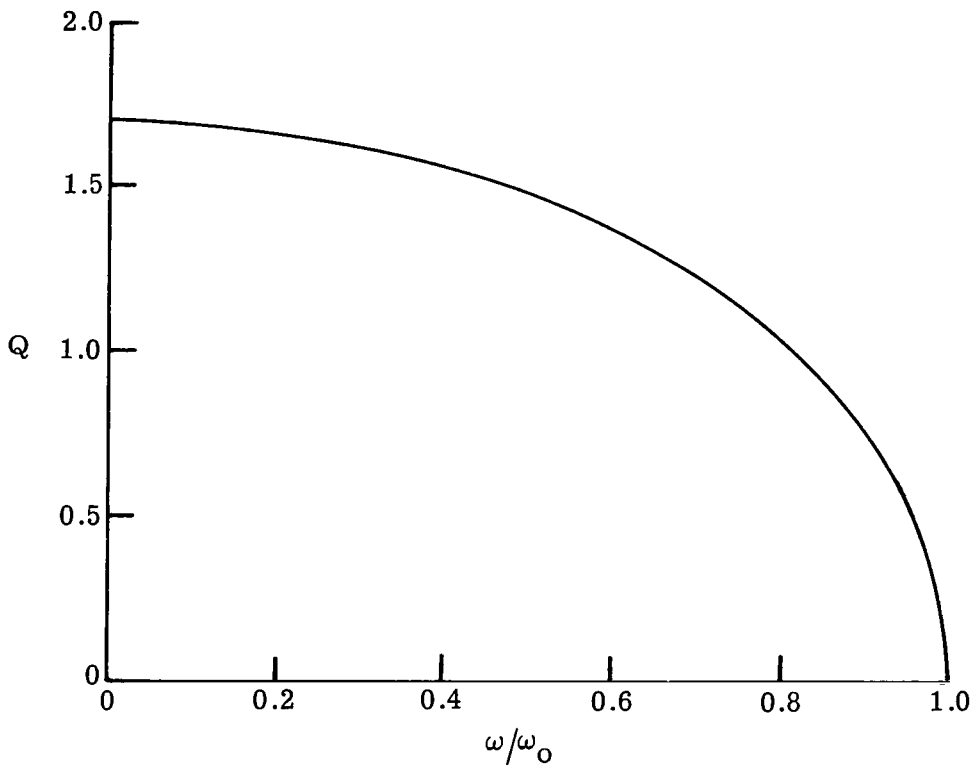

Figure 24.- Variation of $Q = \sigma_r/\sigma_{r,min}$ with ω for the uniformly rotating disk of stars.

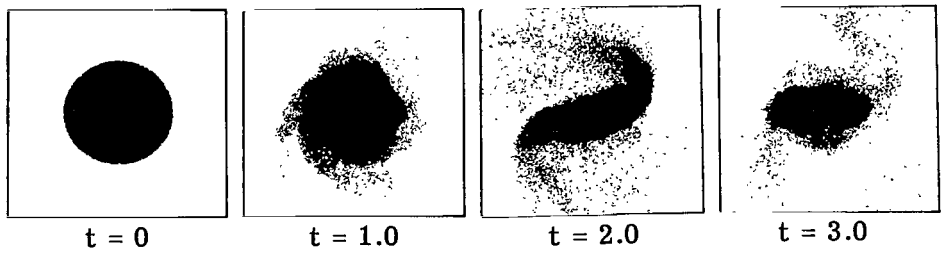

(a) $\omega = 0.8\omega_o$.

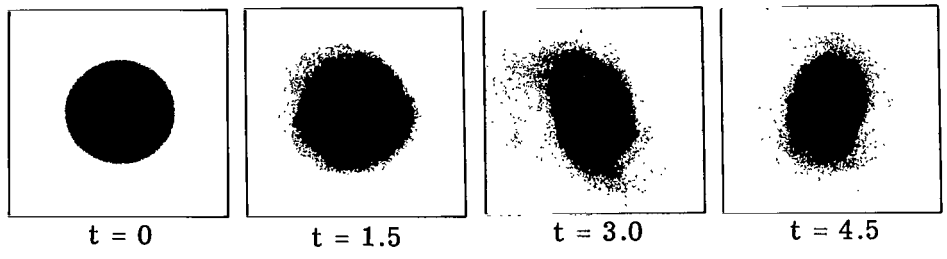

(b) $\omega = 0.6\omega_o$.

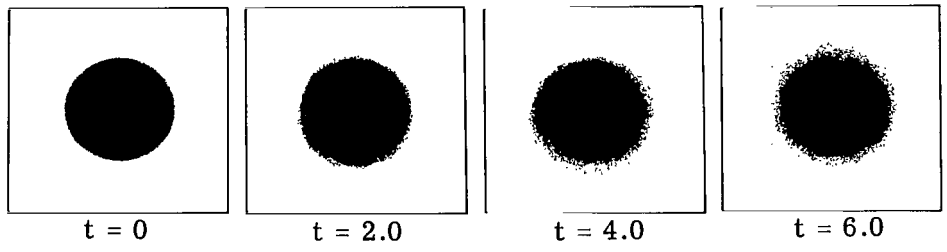

(c) $\omega = 0.4\omega_o$.

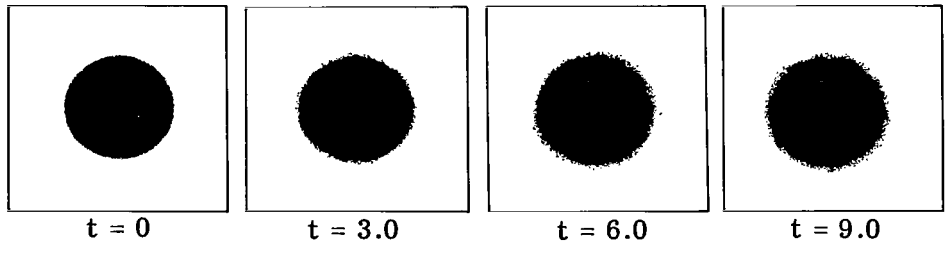

(d) $\omega = 0$.

Figure 25.- Evolution of an initially uniformly rotating and stationary disk galaxy for four values of the angular velocity ω. (ω_o is the angular velocity of the cold (zero-velocity-dispersion) disk).

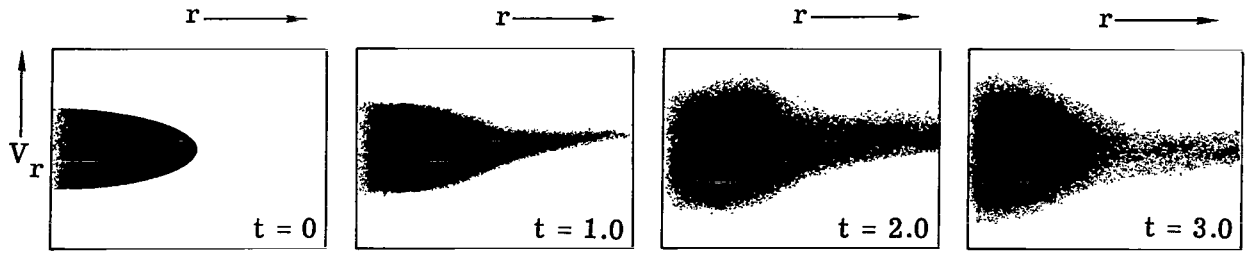

(a) $\omega = 0.8\omega_o$.

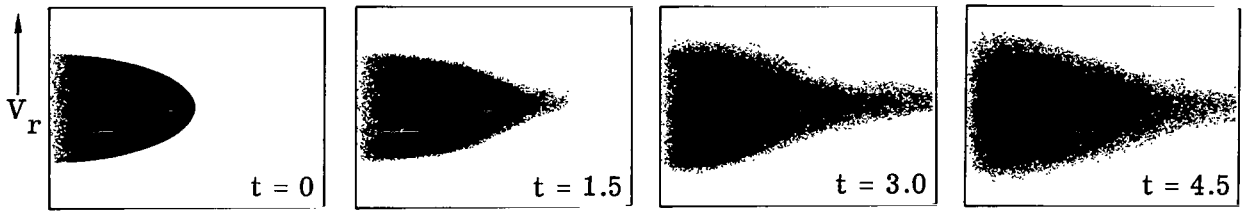

(b) $\omega = 0.6\omega_o$.

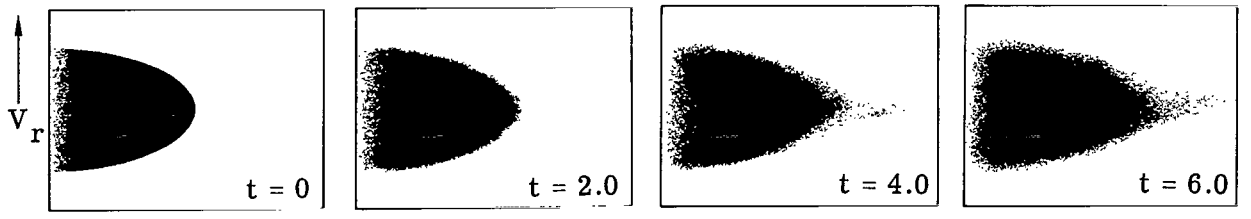

(c) $\omega = 0.4\omega_o$.

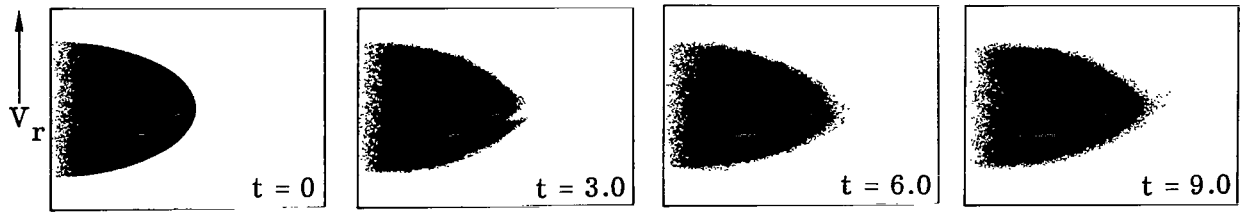

(d) $\omega = 0$.

Figure 26.- Evolution of the radial velocity components of the stars plotted as a function of radius for the four disks shown in figure 25.

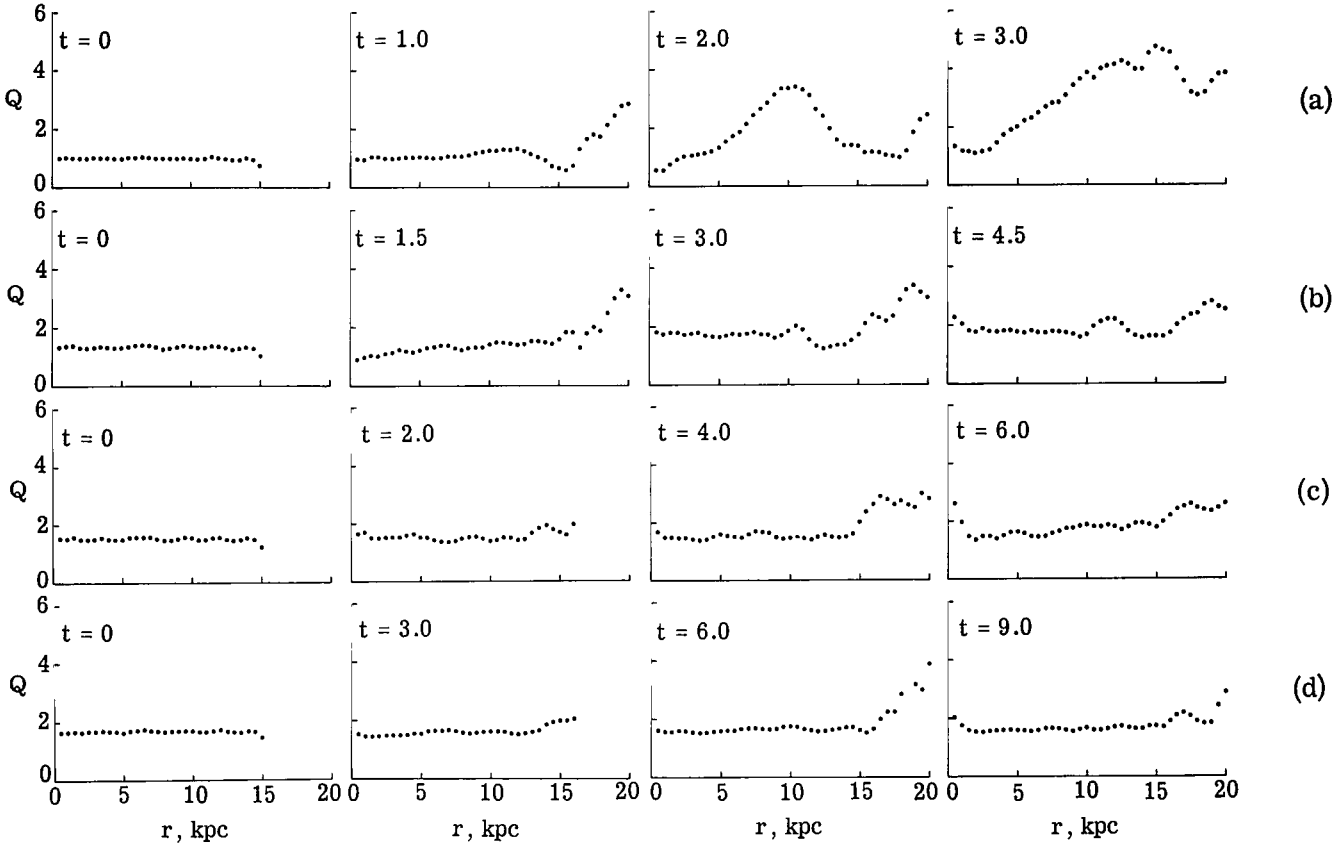

Figure 27.- Evolution of $Q = \sigma_r/\sigma_{r,min}$ for the four disks shown in figure 25 for (a) $\omega = 0.8\omega_o$; (b) $\omega = 0.6\omega_o$; (c) $\omega = 0.4\omega_o$; and (d) $\omega = 0$.

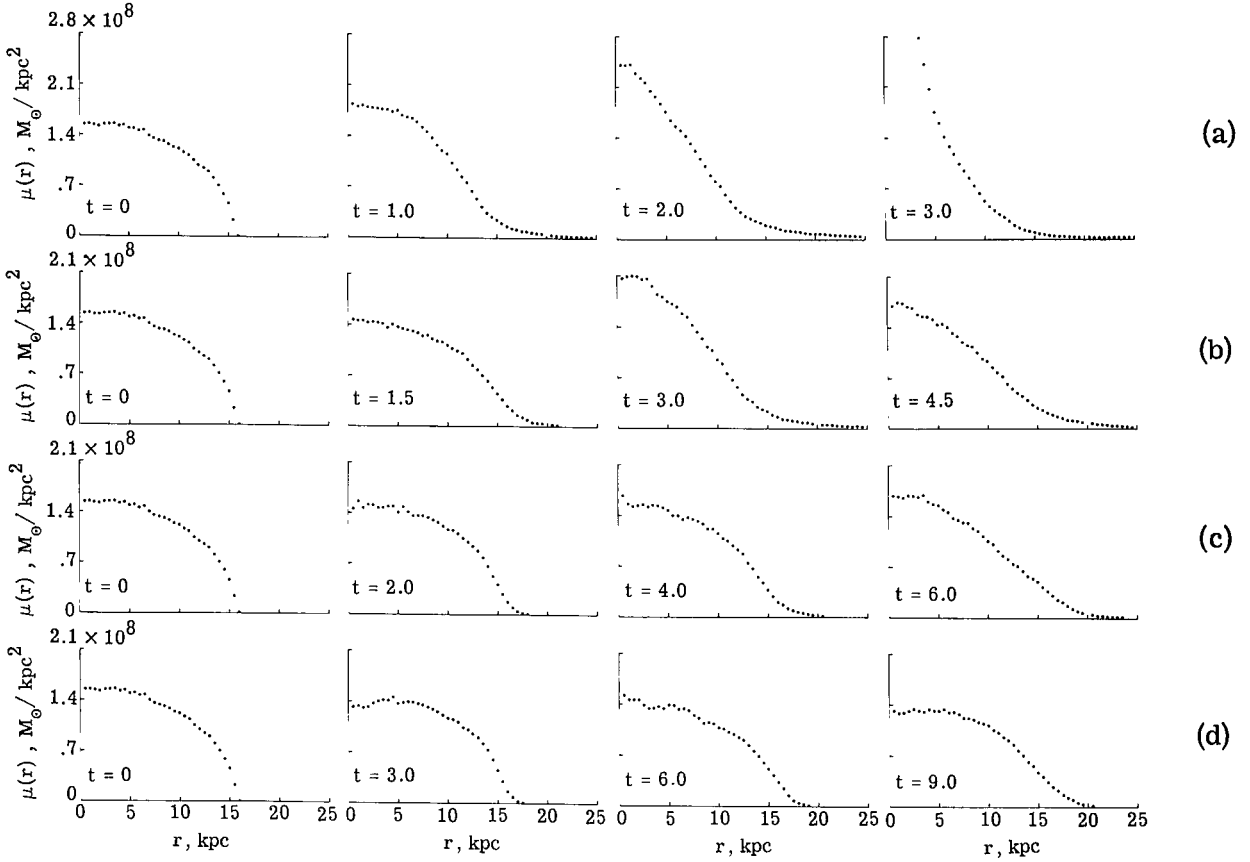

Figure 28.- Evolution of the azimuthally averaged density for the four disks shown in figure 25 for (a) $\omega = 0.8\omega_0$; (b) $\omega = 0.6\omega_0$; (c) $\omega = 0.4\omega_0$; and (d) $\omega = 0$.

025 001 C1 U 30 720317 S00903DS
DEPT OF THE AIR FORCE
AF WEAPONS LAB (AFSC)
TECH LIBRARY/WLOL/
ATTN: E LOU BOWMAN, CHIEF
KIRTLAND AFB NM 87117

"The aeronautical and space activities of the United States shall be conducted so as to contribute . . . to the expansion of human knowledge of phenomena in the atmosphere and space. The Administration shall provide for the widest practicable and appropriate dissemination of information concerning its activities and the results thereof."

— NATIONAL AERONAUTICS AND SPACE ACT OF 1958

NASA SCIENTIFIC AND TECHNICAL PUBLICATIONS

TECHNICAL REPORTS: Scientific and technical information considered important, complete, and a lasting contribution to existing knowledge.

TECHNICAL NOTES: Information less broad in scope but nevertheless of importance as a contribution to existing knowledge.

TECHNICAL MEMORANDUMS: Information receiving limited distribution because of preliminary data, security classification, or other reasons.

CONTRACTOR REPORTS: Scientific and technical information generated under a NASA contract or grant and considered an important contribution to existing knowledge.

TECHNICAL TRANSLATIONS: Information published in a foreign language considered to merit NASA distribution in English.

SPECIAL PUBLICATIONS: Information derived from or of value to NASA activities. Publications include conference proceedings, monographs, data compilations, handbooks, sourcebooks, and special bibliographies.

TECHNOLOGY UTILIZATION PUBLICATIONS: Information on technology used by NASA that may be of particular interest in commercial and other non-aerospace applications. Publications include Tech Briefs, Technology Utilization Reports and Technology Surveys.

Details on the availability of these publications may be obtained from:

SCIENTIFIC AND TECHNICAL INFORMATION OFFICE

NATIONAL AERONAUTICS AND SPACE ADMINISTRATION

Washington, D.C. 20546